

# Surface-Patterned Water Separation Membranes: A Critical Analysis of Current Knowledge and Future Research Needs

Alexander Mitranescu,<sup>#</sup> Maharshi Patel,<sup>#</sup> Stefan Panglisch, Jörg E. Drewes,<sup>\*</sup> and Ibrahim M. A. ElSherbiny<sup>\*</sup>




Cite This: *ACS EST Water* 2024, 4, 5225–5242



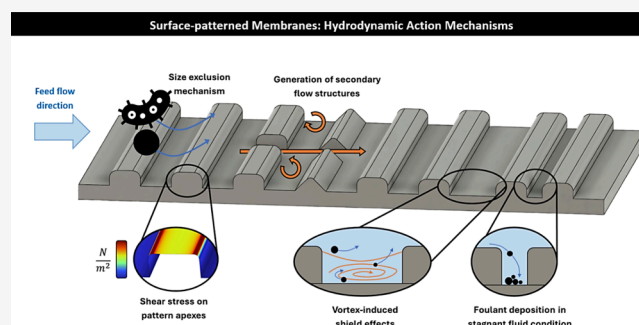
Read Online

ACCESS |

 Metrics & More

 Article Recommendations

**ABSTRACT:** Surface-patterned membranes with engineered nano- and microstructures are emerging as a promising approach to mitigate fouling and enhance membrane performance in water treatment and desalination. This review critically evaluates the current state of research, drawing on findings from over 100 studies to highlight key findings and identify knowledge gaps. A significant research gap persists in understanding the performance of surface-patterned membranes in spacer-filled channels, given their relevance for practical applications. This Perspective provides a summary of critical aspects of key fabrication techniques and relevant characterization methods. In addition, reported performance results are assessed, including effects of fabrication methods on membrane permeability and limitations in scaling and biofouling analyses. By consolidating experimental and numerical outputs, we explored prevailing hydrodynamic theories for surface-patterned membranes in spacer-free channels and their implications for fouling control and hydrodynamic cleaning efficiency. These primary mechanistic effects are often found to be case-specific and occasionally contradictory. Notably, limitations in computational fluid dynamics modeling, often reliant on idealized membrane surfaces, are being discussed with recommendations to achieve improved model accuracy. This review concludes by identifying critical research areas and the needs to advance surface-patterned membranes for sustainable water separation applications.



## 1. INTRODUCTION

It has been more than a decade since the introduction of the first microstructured ultrafiltration hollow fiber membrane in 2010,<sup>1,2</sup> while the microfabrication of polymeric membranes dates back even further to 1988.<sup>3,4</sup> Recently, there has been a growing interest in the development of surface-patterned membranes, featuring regular surface nano- and microstructures, intended as a physical surface modification strategy to mitigate membrane fouling in water treatment and desalination applications. These surface structures are hypothesized to induce mixing effects in the direct membrane vicinity, which were claimed to alter fouling behavior and particle deposition on the membrane surface and, under certain conditions, reduce boundary layer thickness.

To date, over 100 peer-reviewed articles have explored surface-patterned water separation membranes, investigating the performance of various surface patterns in spacer-free channels through bench-scale experiments and/or modeling. While several mechanistic explanations have been proposed in the literature, they are often case-specific and occasionally contradictory.<sup>5–7</sup>

Of the 12 review articles published on this subject between 2017 and early 2024, four reported on surface-patterning

alongside other membrane surface modification techniques and process optimization strategies to reduce membrane fouling,<sup>8–11</sup> while the others focused exclusively on the fabrication and performance of surface-patterned membranes.<sup>12–19</sup> Some reviews primarily discussed fabrication techniques and the manufacturing-structure-performance relationships.<sup>12,16</sup> Others additionally reported on the performance of surface-patterned membranes in bench-scale experiments conducted in spacer-free channels, evaluating pure water permeability (PWP) and common fouling types,<sup>13–15,17</sup> yet without systematically correlating experimental and/or numerical results with the proposed mechanisms of action. One review article focused exclusively on computational fluid dynamics (CFD) modeling.<sup>19</sup>

To the best of our knowledge, a critical assessment of the experimental and numerical methodologies used to evaluate

**Received:** August 21, 2024  
**Revised:** October 30, 2024  
**Accepted:** October 31, 2024  
**Published:** November 14, 2024



**Table 1. Overview of Different Pattern Types (and Pattern Dimensions) That Were Examined for Water Separation Membranes and Their Applicability to Dense and/or Porous Membranes, in Addition to the Type of Fouling That Was Addressed<sup>a</sup>**

Pattern design	Pattern dimensions (height x width x spacing)	Patterns applied to dense/ porous membranes	Fouling type addressed	Ref.
Line-and-space pattern (a, b)*	few - hundreds of nm scale	dense membranes	Inorganic fouling	26,7
	hundreds of nm-few $\mu\text{m}$ scale	porous membranes	Inorganic fouling	45,46
	hundreds of nm-hundreds of $\mu\text{m}$ scale		Organic fouling	47,25,48,49,21,22,50,40,51,52,41
	$\mu\text{m}$ scale		Biofouling	53,42,34,54
	hundreds of nm-few $\mu\text{m}$ scale		Particulate fouling	55,44,56
Discontinuous line pattern (c)	$3 \mu\text{m} \times 2 \mu\text{m} \times 2 \mu\text{m}$	porous membranes	Biofouling	34
Prism pattern (d)*	-	porous membranes	Organic fouling	40,51
	few $\mu\text{m}$ scale		Biofouling	31,57,39
Sharklet triangular pattern (e)	$3 \mu\text{m} \times 2 \mu\text{m} \times 2 \mu\text{m}$	porous	Biofouling	34
Sharklet rectangular pattern (f)	$3 \mu\text{m} \times 2 \mu\text{m} \times 2 \mu\text{m}$	porous membranes	Biofouling	34,35,36,58
	$3 \mu\text{m} \times 2 \mu\text{m} \times 2 \mu\text{m}$		Organic fouling	58
	$3 \mu\text{m} \times 2 \mu\text{m} \times 2 \mu\text{m}$		Particulate fouling	58
Pyramid pattern (g)	few $\mu\text{m}$ scale	porous membranes	Biofouling	31,57,33
	$16 \mu\text{m} \times 25 \mu\text{m} \times 25 \mu\text{m}$		Particulate fouling	29
Reverse pyramid pattern	$16 \mu\text{m} \times 25 \mu\text{m} \times 25 \mu\text{m}$	porous membranes	Particulate fouling	28,29
45°-rotated pyramid pattern	$16 \mu\text{m} \times 25 \mu\text{m} \times 25 \mu\text{m}$	porous membranes	Particulate fouling	29
Pillar pattern (h)	$160 \text{ nm} \times 140 \text{ nm} \times 400 \text{ nm}$	dense membranes	Organic fouling	30
			Biofouling	30
Wave pattern (i)	hundreds of $\mu\text{m}$ scale	porous membranes	Biofouling	23,54,59,60,39,61
	-		Organic fouling	62
Double sinusoidal patterns	-	porous membranes	Organic fouling	63,64
Permeate spacer pattern	hundreds of $\mu\text{m}$ - few mm scale	dense membranes	Inorganic fouling	65,66
	hundreds of $\mu\text{m}$ - few mm scale		Organic fouling	66

<sup>a</sup>Asterisks: numbering (a–i) refers to the respective pattern schematic representation in Figure 1

the performance of surface-patterned membranes has yet to be conducted. For instance, many studies employing CFD modeling have relied on oversimplified representations of membrane surface patterns,<sup>6,20</sup> often assuming them to be ideal and defect-free, although characterization studies have reported anomalies in membrane surface structures.<sup>21–23</sup> Additionally, there remains a significant knowledge gap regarding the mechanistic effects and performance of surface-patterned membranes in spacer-filled channels.

This review aims to complement existing overviews by evaluating the reliability of the current knowledge, assessing the methodologies employed, and identifying key areas for future research to advance our understanding and address existing knowledge gaps. It provides an executive summary on the most critical aspects of the fabrication of porous and dense patterned membranes, emphasizing their scalability and applicability to various complex membrane structures. It, briefly, addresses the characterization methods, focusing on relevant parameters for surface-patterned membranes and critically discusses the performance results. Furthermore, it evaluates methodologies employed in bench-scale experiments, particularly concerning scaling and biofouling (two common fouling types in continuous full-scale operations) and provides detailed recommendations on the improvement of these methods.

Additionally, this review provides a critical evaluation of CFD modeling (methods and results) for surface-patterned

membranes, offering comprehensive recommendations to enhance the accuracy of these numerical models. By compiling results from both experimental and numerical studies, it presents an overview of prevailing theories in the literature regarding the primary hydrodynamic mechanisms that govern the antifouling behavior of surface-patterned membranes. It also explores the impact of surface-patterning on the hydrodynamic cleaning efficiency, a research topic that has received limited attention in the literature. In conclusion, this review article identifies key areas for further research and outlines critical research topics and knowledge gaps that require intensified investigations to advance the application of surface-patterned water separation membranes.

## 2. PREPARATION OF PATTERNED MEMBRANES

**2.1. Membrane Surface Pattern Design.** Previous studies have explored a variety of surface topographies with different shapes. Commonly investigated patterns include regularly repeating intervals, such as lines-and-spaces with rectangular, triangular, semicircular, and trapezoidal cross sections.<sup>21,22,24–27</sup> Recently, more complex surface patterns have been examined, including discontinuous lines, pyramids, inverted pyramids, pyramids at 45-degree angles, and pillars with circular to square cross sections.<sup>28–33</sup> Pushing the boundaries further, researchers have incorporated nature-inspired antifouling bionic patterns onto membrane surfaces. Noteworthy examples include mimicking the distinctive

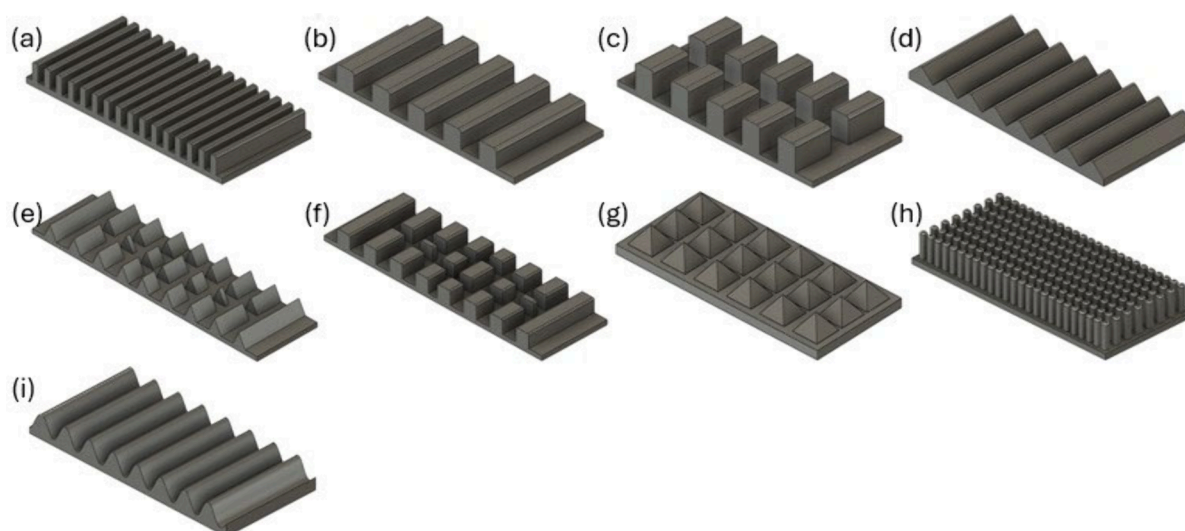


**Figure 1.** Different pattern designs employed to produce patterned membranes: (a) line-and-space pattern at the nm scale, (b) line-and-space pattern at the  $\mu\text{m}$  scale, (c) discontinuous lines pattern, (d) prism pattern, (e) Sharklet triangular pattern, (f) Sharklet rectangular pattern, (g) pyramid pattern, (h) pillar pattern, and (i) waves pattern.

**Table 2.** Overview of the Surface-Patterning Methods Reported in the Literature Alongside the Type of Pattern Shapes to Be Realized, Applicability to Porous and Dense Polymeric Membranes, and the Pattern Height Fidelity<sup>a</sup>

Patterning method	Pattern shape	Applicability of patterning method to dense/porous membranes	Pattern height fidelity (%) <sup>*</sup>	Ref.
Phase separation micro-molding	Sharklet triangular pattern	porous membranes	75	34
	Sharklet rectangular pattern	porous membranes	75 <sup>34-95</sup> <sup>58</sup>	34, 35, 36, 58
	Line-and-space pattern	porous membranes	28 <sup>22-98</sup> <sup>53</sup>	53, 46, 27, 49, 35, 21, 50, 40, 51, 52, 22
	Discontinuous lines pattern	porous membranes	75	34
	Prism pattern	porous membranes	45 <sup>51-91</sup> <sup>57</sup>	31, 57, 40, 51, 39
	Pyramid pattern	porous membranes	91 <sup>57-100</sup> <sup>29</sup>	31, 57, 29, 33
	Reverse Pyramid patten	porous membranes	100	28, 29
	45°-rotated pyramid pattern	porous membranes	100	29
	Wave pattern	porous membranes	9 <sup>23-73</sup> <sup>59</sup>	23, 59, 60, 39, 61
	Pillar pattern	porous membranes	-	32
Nanoimprinting lithography	Line-and-space pattern	dense membranes	31 <sup>7-34</sup> <sup>26</sup>	26, 71, 7
	Line-and-space pattern	porous membranes	11 <sup>69-100</sup> <sup>48</sup>	47, 55, 44, 45, 69, 70, 46, 25, 48, 56, 77
	Wave pattern	porous membranes	-	54
<b>Other patterning methods</b>				
Sol-gel based nanoimprinting	Pillar pattern	dense membranes	-	30
Imprinted by permeate spacer	Spacer pattern	dense membranes	-	66, 65
3D-Printing	Double sinusoidal pattern	porous membranes	-	63, 64
	Wave pattern	porous membranes	-	62
	Line-and-space pattern	porous membranes	100	41, 80
Photo lithography	Line-and-space pattern	porous membranes	100	42

<sup>a</sup>Asterisks: pattern height fidelity is the ratio of the actual pattern height achieved on the membrane surface to the pattern height on the master mold.<sup>68</sup>

Sharklet pattern.<sup>34–38</sup> The pattern features were incorporated into membrane coupons, ranging in size from millimeters to square centimeters. An overview of all employed surface patterns for water separation membranes, along with their dimensions and schematic representations, is provided in Table 1 and Figure 1, respectively.

The reported antifouling performance of surface-patterned membranes is primarily attributed to the promotion of hydrodynamic conditions at the membrane surface affecting

interactions between feed components (e.g., biofoulants and particles) and the membrane surface patterns. Critically, the pattern designs described in the literature can be classified into two categories: relatively simple 3D structures (e.g., lines-and-spaces, prism) inducing vortices and shear stress and more complex 3D structures also capable of generating secondary flows (e.g., Sharklet). Extensive efforts were devoted to determining the optimal configuration with respect to different pattern shapes and dimensions on impacting antifouling

behavior.<sup>29,31,34,39,40</sup> For instance, Choi et al. examined the biofouling propensity for dense membranes with surface pattern shapes, including lines-and-spaces, discontinuous lines, and Sharklet patterns (with rectangular or triangular cross sections).<sup>34</sup> Similarly, Zhao et al. tested wave-, triangular-, rectangular-, and trapezoidal-shaped line patterned polysulfone membranes for the harvesting of microalgae biomass.<sup>39</sup>

Furthermore, the pattern dimensions (i.e., height of features, spacing between features) were found to be of great importance.<sup>35,41,42</sup> For example, Choi et al. observed a size exclusion mechanism that influenced the antifouling performance of reverse osmosis (RO) membranes with nanoscale pillars that reduces the contact area for attachment of micrometer-scale bacteria.<sup>30</sup> In a recent publication, Ng et al. reported that an increased ratio of latex particle size ( $a$ ) to unit spacing ( $s$ ) over height ( $h$ ), ( $a/(s/h)$ ), was indicative of a higher fouling tendency for a 3D printed ceramic membrane.<sup>41</sup> Additionally, the height of surface features (i.e., structures) was found to have a greater impact on the antifouling performance than the width of the patterns. In another comprehensive study by Maruf et al., colloidal filtration experiments using surface-patterned UF membranes revealed that increasing the pattern height could be more effective in enhancing the back diffusion of colloidal silica particles. This was indicated by higher measured critical flux values (i.e., the flux at which the flux-transmembrane pressure correlation starts to deviate from linearity, indicating the onset of fouling<sup>43</sup>) and increased calculated shear-induced diffusivity.<sup>44</sup>

Despite the lack of direct experimental evidence of how dimensions of membrane surface patterns affect the deposition mechanism of foulants and particles, understanding the effects of pattern shape and feature dimensions on fluid dynamics is essential. This fundamental knowledge is critical for the effective optimization of surface pattern designs to improve membrane performance and tackle specific challenges encountered in practical settings (i.e., feed-channel pressure drop (FCPD)).

**2.2. Methods for Preparation of Surface-Patterned Polymeric Membranes: Strategies for Porous and Dense Membranes.** Many physical microfabrication methods, based on soft lithography and nanoimprinting lithography, have been investigated in previous studies for transferring both simple and complex patterns onto the surfaces of polymeric membranes, including flat-sheet and hollow fiber membranes as well as porous and dense membranes. As aforementioned, some review articles provide detailed accounts of these preparation strategies.<sup>12,13,15,16</sup> However, in this review, we provide only a brief conceptual overview of these methods. Table 2 provides an overview of patterning methods used in previous studies reported in the peer-reviewed literature, detailing pattern shapes, applicability to porous and dense membranes, and the quality of patterning (quantified by pattern height fidelity,%).

**2.2.1. Surface Patterning Methods for Porous Membranes.** As summarized in Table 2, both phase separation micromolding (PS $\mu$ M)<sup>10,22,23,34–36,46,51,59,67,68</sup> and nanoimprinting lithography (NIL)<sup>7,17,26,45,46,55,69–72</sup> are frequently employed physical surface alteration methods for preparing porous surface-patterned membranes. PS $\mu$ M is a lithographic method that utilizes the polymer phase-inversion process and can employ a wide range of polymer materials to prepare surface patterned membranes with various surface top-

ographies, aspect ratios, pore sizes, and porosities.<sup>46,56,68</sup> Nonsolvent liquid-induced PS $\mu$ M (LIPS $\mu$ M), using solid molds (e.g., silicon mold), is considered the state-of-the-art.<sup>73</sup> Later, vapor-induced PS $\mu$ M (VIPS $\mu$ M) has been developed to overcome a major obstacle of LIPS $\mu$ M, where the phase separation is induced from the nonstructured (bottom) side, resulting in a hierarchical pore size gradient across the surface-patterned porous membrane, where the selective side is located on the bottom of the membrane.<sup>31,53,68</sup> In VIPS $\mu$ M, the nonsolvent component (e.g., water) is introduced in the vapor phase (as typically occurs in the VIPS process) through water vapor-permeable molds made of polydimethylsiloxane (PDMS).<sup>74</sup> The pattern fidelity and pore structures of surface-patterned membranes can be controlled by optimizing specific parameters that influence the nonsolvent diffusion rate into the cast film, including exposure time to water vapor, mold thickness, gap (film) thickness, and casting solution composition.<sup>68</sup> PS $\mu$ M methods have other limitations due to polymer film shrinkage and the difficulty of detaching the film from the mold. Consequently, this method is particularly effective for replicating molds with a high aspect ratio.<sup>5,73</sup>

Won et al. developed a modified soft-lithographic method to address the primary limitations of PS $\mu$ M methods, known as the modified immersion-precipitation method.<sup>31</sup> This method shifts the interface where phase separation is initiated from the bottom side of the polymer film to the top side by placing a nonwoven fabric on the cast polymer film prior to immersion in the coagulation bath. Additionally, the study highlighted the effects of polymer material molecular weight cutoff (MWCO) and mold material type on the fidelity of the surface-patterned porous membranes.

Spray-modified nonsolvent induced phase separation (s-NIPS) is another modified technique for producing polymeric membranes by immediately spraying a nonsolvent directly after the film casting, rapidly solidifying the polymer.<sup>21–23,40,51,52,59,75,76</sup> This technique was employed by Ilyas et al. and Marbelia et al. to create surface-patterned porous membranes, testing various solvent, nonsolvents, polymer types, and additives.<sup>21,22,51</sup>

NIL is the main alternative method to PS $\mu$ M and other soft lithographic methods, and it is the most suitable for upscaling into technical and industrial scales.<sup>77</sup> NIL is a straightforward surface patterning method for polymeric membranes that combines two mechanistic effects: “direct thermal embossing” and “compression molding”.<sup>78,79</sup> The molds are made of mechanically stable materials, e.g., silicon and metals. The membrane surface patterning mechanism is occurring through pressure-induced viscoelastic deformation at the membrane area in direct contact with the mold at temperatures below the glass transition temperature ( $T_g$ ), resulting in the squeeze flow of the viscous polymer into the mold cavities.<sup>17,55,69</sup> High patterning resolution (sub-10 nm features) can be achieved by optimizing three major parameters: temperature, pressure, and time. The influences of these parameters on patterning fidelity have been investigated in detail.<sup>25,26,69,71</sup> Optimal patterns were found to be achieved with a pressure magnitude between the yield stress and densification stress of the membrane material.<sup>69</sup>

Similar to the NIL mechanism, microimprinting lithography (MIL) has been successfully employed for replicating micrometer-scale line-and-space patterns onto the surfaces of polyether sulfone microfiltration and ultrafiltration mem-

brane.<sup>46,56</sup> Furthermore, the upscaling of the NIL mechanism to a technical scale has been investigated through roll-to-roll nanoimprint lithography of ultrafiltration membranes.<sup>77</sup>

Furthermore, surface-patterned membranes have recently been created by using 3D printing techniques. Two approaches are reported in the literature. The first approach involves depositing a selective polymer layer on top of a 3D-printed support structure.<sup>62–64</sup> The second approach involves preparing an alumina ink containing Al<sub>2</sub>O<sub>3</sub> powder with a binder. A gradient porous structure is formed by using dip coating and spin coating for different layers with varying particle sizes, followed by partial solidification. This membrane is then 3D-printed with the same ink, solidified at room temperature, and sintered at a high temperature to complete the fabrication of a patterned ceramic membrane.<sup>41,80</sup>

### 2.2.2. Surface Patterning Methods for Dense Membranes.

In contrast to porous membranes, direct patterning of dense thin-film composite (TFC) membranes via thermal embossing methods using hard stamps has always been challenging because TFC membranes are subjected to significant plastic deformation, which can damage the cross-linked polyamide layer and adversely impact permselectivity. Furthermore, the achievable depth of surface features is limited (compared with other methods, such as PS $\mu$ M), potentially restricting the benefits of surface patterning. To date, the most reliable method for preparing surface-patterned TFC membranes involves a two-step approach: surface patterning of the porous membrane support followed by conventional interfacial polymerization.<sup>5,25,45,46,56,70</sup> ElSherbiny et al. compared surface-patterned TFC membranes prepared on patterned macroporous polyether sulfone membrane supports using both the MIL and PS $\mu$ M methods.<sup>46</sup>

The two-step approach offers flexibility regarding the employed methods, better control over surface pattern fidelity, and the ability to fine-tune the intrinsic characteristics of each layer individually. However, a significant drawback of surface-patterned TFC membranes prepared through conventional interfacial polymerization is the uncontrolled thickness of the polyamide layer on the surface structures, which might affect the intrinsic permselective properties. It has been observed that the polyamide layer thickness varies considerably, with greater thickness in the valley regions compared to the apex regions.<sup>45,46</sup> Another limitation of the conventional interfacial polymerization method is the varying roughness scales for the resulting composite structures, i.e., nanoscale roughness of the polyamide layer and the larger roughness scale of the underlying patterned membrane support (typically ranging from a few hundred nanometers to a few micrometers). These intricate roughness scales are often overlooked in the literature, despite their potential to significantly impact membrane-solute and membrane-foulants interactions and, consequently, overall membrane performance.

Recently, unconventional interfacial polymerization methods have been proposed to fabricate a uniform, conformal, thin polyamide selective layer over patterned porous membrane supports. For instance, Choi et al. introduced a layered interfacial polymerization method,<sup>34,81</sup> in which a thin polyelectrolyte bilayer (~10 nm) was electrostatically assembled on a prehydrolyzed polyacrylonitrile patterned support. This interlayer blocked the support pores and provided a base for the subsequent polyamide layer. Another alternative method, namely spin-drying assisted interfacial polymerization, was recently introduced by Ilyas et al.,<sup>76</sup> where

a spinning technique was employed during an interfacial polymerization process to remove excess diamine solution from the microstructures, enhancing the characteristics of the formed polyamide layer.

Furthermore, there are two unconventional interfacial polymerization methods, dual-layer slot coating,<sup>82</sup> and an electrospray technique,<sup>83,84</sup> which have been successfully employed to prepare a polyamide layer atop polydopamine precoated flat substrates. These methods can also be promising to overcome the limitations of conventional interfacial polymerization and fabricate a uniform, conformal selective polyamide layer on patterned membrane supports.

On the other hand, Weinman et al. investigated the applicability of the direct patterning thermal embossing method on a series of commercial RO and nanofiltration (NF) TFC membranes using silicon stamps with regular line-and-space nanopatterns.<sup>26</sup> For all membranes, the imprinting conditions were adapted to ensure that the local strain applied to the polyamide layer remained below the onset of cracking.<sup>71,85</sup> Additionally, thermal-embossing-assisted micro-patterning lithography was investigated for the direct patterning of commercial brackish TFC membranes. However, the produced membranes experienced significant and largely irreversible compaction, which affected their permeance.<sup>86</sup> Overall, the successful direct patterning of dense TFC membranes via thermal embossing requires an appropriate consideration of several factors. The size and design of the surface patterns must align with the intrinsic properties of the polyamide film (e.g., film thickness). The imprinting conditions must be sufficiently robust to achieve the desired pattern depth while being controlled to prevent exceeding the onset of cracking of the polyamide film and to avoid significant layer compaction.

### 2.3. On the Characterization of Surface-Patterned Membranes.

In principle, all well-established characterization methods that are used for conventional flat-sheet water separation membranes are also relevant and applicable to surface-patterned membranes. Generally, the characterization parameters are classified into membrane chemistry and material structure-related parameters (i.e., surface/bulk chemical structure, mechanical properties, surface charge, membrane affinity, thermal properties), membrane porous structure and morphology-related parameters (i.e., pore size distribution, porosity, membrane morphology, surface roughness, barrier thickness), and membrane perm-selectivity and barrier-related parameters (i.e., membrane permeability, retention, selectivity, MWCO). While these well-established methods were thoroughly discussed in previous review articles,<sup>87,88</sup> the impacts of surface-patterning on certain characterization parameters have not been properly studied and understood. For instance, a few studies reported on different measured zeta-potential values (i.e., membrane surface charge) for surface-patterned TFC membranes, compared to flat TFC membranes.<sup>46,56</sup> This was related to certain topographically induced effects on the measured zeta-potential. However, there have been no dedicated experimental studies providing a reliable interpretation of this phenomenon. A similar research gap exists regarding the impact of surface-patterning on membrane affinity measurements.

Additionally, there are specific characterization parameters relevant to surface-patterned membranes, which are “pattern height fidelity” and an “increase in the membrane active surface area”. These parameters require fine topographical surface

characterization using techniques such as optical profilometry or atomic force microscopy, which provide high-resolution 3D images of the patterned membrane surface.

Pattern height fidelity is a key morphological parameter that characterizes the extent of the membrane surface topographical modification, and hence, it evaluates the surface-patterning quality. It is defined as the ratio of the actual pattern height achieved on the membrane surface to the pattern height on the master mold.<sup>68</sup> Table 2 lists the general ranges for pattern height fidelity for surface-patterned membranes produced by different fabrication methods. It is worth mentioning for those studies where pattern height fidelity was not quantified, the values in Table 2 were estimated based on the available information on the mold dimensions and the actual surface patterns.

The increase in membrane active surface area is another characterization parameter for surface-patterned membranes, which quantifies the improvement in the membrane active surface area due to the surface-patterning. A correlation between the increase in membrane active surface area and enhanced membrane performance, particularly pure water permeability<sup>6,46</sup> and antifouling propensity,<sup>56</sup> was reported in literature. The increase in membrane active surface area can be quantified using two methods: one is based on atomic force microscopy (AFM),<sup>46</sup> and the other is combining optical profilometer and calculation software (such as ImageJ). However, no standardized method has been developed in the literature.

### 3. CRITICAL ASSESSMENT OF THE CURRENT KNOWLEDGE ON THE EFFECTS OF SURFACE-PATTERNING ON KEY PERFORMANCE PARAMETERS

Extensive research has been conducted to investigate the impacts of surface patterning on the performance of water separation membranes. Routine performance testing has included measuring pure water permeability (PWP) and solute retention as well as examining the tendencies for concentration polarization and various fouling types. Surface-patterned membranes were compared to either flat-sheet membranes (for those prepared by soft lithographic methods) or flat-compact membranes (for those prepared by thermal embossing methods). In this section, the performance results of surface-patterned membranes are critically compared to understand the different effects of surface patterning on typical membrane performance parameters. Furthermore, the experimental methods used for examining specific fouling types are critically assessed, and recommendations for potential improvements are provided.

A critical review of the literature reveals that surface-patterning methods frequently lead to certain alteration in most performance-affecting structural and physicochemical properties (e.g., pore size distribution, surface porosity, membrane affinity, and mechanical properties). These changes complicate efforts to fully understand the individual effects of surface patterning on membrane performance and the underlying mechanisms of action since the measured performance is influenced not only by the surface patterns but also the characteristics of all membrane layers.

Decoupling these effects through optimization of surface-patterning or fabrication methods is highly challenging because of the inherent limitations of these methods (cf. Section 2).

However, this challenge can potentially be addressed by developing membrane testing or fluid characterization methods that can help in elucidating the impacts of membrane structure from those of surface patterning, thereby allowing a clearer assessment of individual contributions to membrane performance. These methods should focus on the mechanistic effects or performance parameters (such as antifouling behavior) due to membrane surface-patterning. Hence, standard permeation tests should be avoided.

One relevant practical approach could involve using Particle Image Velocimetry (PIV) to investigate the effects of surface patterns on hydrodynamics in the feed-retentate channel.<sup>86</sup> Another example is the investigation of biofilm formation on membranes under crossflow conditions (without permeation). Furthermore, these coupled effects can be separated using numerical simulations, providing further insight into the specific role of surface patterning in membrane performance.

**3.1. Effects of Surface Patterning on Pure Water Permeability.** The impact of surface patterning on PWP is influenced by various parameters, including polymer material properties,<sup>24,26,45</sup> casting solution composition,<sup>21–23,51</sup> membrane surface properties,<sup>23,34,54,71</sup> porous structure,<sup>25,31,53,70</sup> testing conditions (e.g., crossflow velocity),<sup>63</sup> and the patterning method used.<sup>46</sup> To better understand these effects, it is essential to classify previous research published in the peer-reviewed literature based on the types of membranes, specifically porous and dense membranes.

**3.1.1. Effects for Porous Membranes.** Patterned porous membranes typically exhibit enhanced PWP due to the enlarged membranes active surface area,<sup>28,29,31,40,51</sup> regardless of the pattern shape and patterning method. However, Marbelia et al. reported a negative effect on PWP during the production of patterned membranes using a modified phase inversion method and casting solutions with certain polymer concentrations, which was attributed to the reduction of cavities.<sup>22</sup> Additionally, they claimed to achieve both a larger average pore diameter and secondary pore size through nonsolvent spraying, which could further increase PWP.

The effect of nonsolvent spraying on membrane performance was also observed by Zhao et al., who noted that wave-patterned membranes were more permeable than their flat counterparts.<sup>39</sup> They also studied the effect of adding polyethylene glycol (PEG) to the casting solution, which slowed down the precipitation rate due to increased viscosity, resulting in more porous (open) membranes and increased PWP. However, this mechanism only worked up to a certain PEG concentration.<sup>61</sup>

Furthermore, for patterned membranes prepared by NIL, Maruf et al. reported a decrease in the MWCO, implying a densification of the membrane porous structure due to the compression molding mechanism.<sup>44,47</sup> Interestingly, this did not result in reduced PWP, leading the authors to conclude that although densification could reduce permeation, the simultaneous enhancement in permeation due to the increased membrane active surface area could act as a counteracting mechanism.<sup>47,55</sup>

**3.1.2. Effects for Dense Membranes.** In 2016, Weinman et al. reported the first attempt for direct patterning of dense membranes using the thermal embossing method.<sup>26</sup> They observed no significant change in PWP and concluded that surface patterning does not inherently damage the membrane. This was further supported by Ward et al.<sup>7</sup> However, in a later systematic study, Weinman et al. examined PWP for 13

commercial dense membranes subjected to thermal embossing using flat metal stamps and patterned metal molds with line-and-space patterns.<sup>71</sup> Five TFC membranes experienced a decrease in PWP due to the compaction effect, while the other eight TFC membranes maintained a statistically unchanged PWP. However, the concept of membrane active surface area enhancement and its impact on PWP were not considered.

In contrast, recent studies reported increased PWP for surface-patterned TFC membranes prepared via *in situ* direct permeate spacer imprinting.<sup>65,66</sup> Additionally, surface-patterned TFC membranes prepared by the two-step approach (cf. section 2.2.2) were reported to exhibit higher PWP compared to flat-compacted TFC membranes, at identical conditions, due to the enhanced membrane active surface area.<sup>45</sup> Furthermore, Rickman et al. reported that patterned TFC membranes are more likely to stabilize sooner than flat TFC membranes because of the precompaction condition of the microporous substrate during the nanoimprinting process.<sup>25</sup> Interesting insights regarding the enhancement of PWP for Sharklet-patterned TFC membranes via controlling the porosity and pore size of the porous substrates were reported by Choi et al.<sup>34–36</sup> ElSherbiny et al. conducted a compelling study comparing the preparation methods and the performance of surface-patterned TFC membranes prepared employing PS $\mu$ M and MIL methods.<sup>46</sup> The study claimed that the increased PWP for surface-patterned TFC membranes was due to the increased membrane active surface area as well as the promoted hydrophilicity.

In conclusion, the increase in PWP due to surface patterning in both dense and porous membranes is fundamentally attributed to the increased membrane active surface area. However, this effect is also significantly dependent on the type of membrane, polymer material, porous structure, and patterning method employed.

**3.2. Effects of Surface Patterning on Salt Retention and Concentration Polarization.** Generally speaking, the salt retention performance of surface-patterned dense membranes has been used as an indication of the integrity of the polyamide layer while successfully applying the surface-patterning process.<sup>34–36,71</sup> Surface-patterned TFC membranes were tested using NaCl<sup>25,30,34–36,45,70</sup> and bivalent salts (e.g., MgSO<sub>4</sub>, CaCl<sub>2</sub>)<sup>50,65,66,71</sup> in both crossflow and dead-end filtration modes, and their performance was compared with their flat counterparts. Interestingly, the influence of the alignment of membrane surface patterns with respect to feed flow direction was also considered.<sup>26,71,46</sup> The rationale is that surface patterned membranes can influence the hydrodynamics in the membrane vicinity, enhancing back-diffusion and reducing the boundary layer thickness and osmotic pressure.<sup>46</sup>

For instance, direct patterning of commercial TFC membranes was accompanied by a certain decay in MgSO<sub>4</sub> retention for some membranes, which was attributed to the damage of the polyamide layer due to the excessive viscoelastic deformation during thermal embossing. However, the other ten surface-patterned TFC membranes exhibited almost similar salt rejection as the flat-sheet membrane, indicating an intact polyamide selective layer.<sup>71</sup>

Additionally, a number of modeling and experimental studies have examined the impacts of surface patterning on concentration polarization; the modeling studies are reviewed in Section 4.3. Maruf et al. conducted salt retention experiments using NaCl and CaCl<sub>2</sub> feeds at a concentration of 1,000 mg/L. Their findings showed that patterned TFC

membranes induced back diffusion of retained salts into the bulk solution, leading to a reduction in concentration polarization.<sup>45</sup> This was attributed to certain alterations in feed flow profiles near the membrane surface, which generated localized turbulence and shear stress forces. These effects were found to depend on key operating conditions, cross-flow velocity, dimensions of surface structures, and the orientation of surface patterns relative to the feed flow direction.

Furthermore, ElSherbiny et al. conducted extensive NaCl retention experiments at concentrations of 2000 and 10,000 mg/L under various operating conditions in a spacer-free channel. The filtration system was initially set to turbulent conditions. They reported that surface-patterned TFC membranes experienced less concentration polarization compared to typical flat-sheet TFC membranes, due to the formation of vortices and shear stresses.<sup>46</sup> Additionally, surface-patterned TFC membranes installed parallel to the feed flow direction developed a thinner boundary layer compared with those installed perpendicular to the flow.

However, a comprehensive simulation study by Zhou et al. investigating different pattern shapes in a spacer-free flow channel presented contradictory results regarding the effects of surface patterning on key performance parameters, including concentration polarization.<sup>6</sup> This study reported that surface patterns increased concentration polarization compared with flat-sheet membranes, with the increase being linearly proportional to the height of the patterns. Zhou et al. also challenged the claims of reduced concentration polarization for patterned membranes due to vortices,<sup>45,46</sup> arguing that in the laminar regime the vortices formed lacked sufficient velocity to effectively scour the membrane.<sup>6,7</sup>

In summary, surface patterning may not significantly influence membrane selectivity (expressed as salt rejection). However, there are conflicting results regarding the impacts of patterning on the concentration polarization. This discrepancy may stem from factors such as improper experimental design, ineffective modeling, and extensive simplification of the influencing parameters. These varied results highlight the need for further analysis to better understand the effects of surface patterning on concentration polarization. Additionally, feed spacers, that are a key factor for the flow characteristics and concentration polarization in membrane feed channels in commercial-scale membrane modules,<sup>89</sup> were not yet considered in previous studies.

### 3.3. Effects of Surface Patterning on Scaling Propensity and Potential Methodology Improvements.

There is limited information in the peer-reviewed literature on the impacts of surface patterning on scaling, a major fouling phenomenon in spiral wound modules (SWM). One key study was conducted by Maruf et al.,<sup>45</sup> where bench-scale dead-end scaling experiments were performed at a constant pressure using CaSO<sub>4</sub> at a concentration of 1,000 mg/L. They found that gypsum crystals precipitated faster on surface-patterned membranes than on flat-sheet membranes, indicating an earlier onset of fouling. This was attributed to higher fluxes in patterned membranes, which led to faster saturation of CaSO<sub>4</sub>. Furthermore, the morphology of the gypsum crystals formed on the patterned membranes differed from those on flat-sheet membranes, making them easier to remove through forward flushing. This improved cleanability was attributed to the enhanced hydrodynamic conditions on the surface-patterned TFC membrane.

Further research is certainly needed to investigate the impacts of surface-patterning on relevant scaling types. These experimental studies should be properly designed to simulate industrial-scale operating conditions, particularly the cross-flow mode and application of feed spacers, and to explore different plug flow operation modes. Moreover, these experiments should incorporate the concept of *in situ* scale formation,<sup>90</sup> as surface-patterned membranes have been found to influence hydrodynamics in the membrane vicinity and particle deposition behavior, which may result in different scaling mechanisms compared to flat-sheet membranes. Experimental procedures should also decouple the effects of concentration polarization and scaling on membrane performance. Additionally, early and accurate detection of membrane scaling is critical for a comprehensive understanding of the effects of surface patterns on the onset of fouling. It is also recommended to use constant flux filtration, which enables consistent comparisons between membranes with varying permselective properties.

**3.4. Effects of Surface Patterning on Particulate Fouling Propensity.** To understand the transport and deposition patterns of particulate foulants on the membrane surface, experiments using natural or model particulate foulants are usually conducted. Consequently, several studies in the literature investigated the effects of surface patterning on particulate fouling propensity under different testing conditions, using PMMA,<sup>91,92</sup> polystyrene,<sup>20,93</sup> or silica<sup>44,56</sup> model foulants at the micrometer<sup>29,91</sup> and nanometer<sup>94,95</sup> scale. However, none of these studies were conducted in the presence of a feed spacer despite its crucial effect on flow characteristics in the membrane channel.

One key finding from these experiments was the preferential deposition of particles in the valleys, rather than the apexes of the patterns on UF and TFC membranes, that is well-documented by scanning electron microscope (SEM) micrographs<sup>56,91,92</sup> and confocal laser scanning microscopy (CLSM)<sup>20</sup> images. Additionally, lower overall mass deposition<sup>20,29,93</sup> and lower overall surface coverage<sup>94</sup> of model particles on surface-patterned compared to nonpatterned flat-sheet UF<sup>20,29,93</sup> and TFC<sup>94</sup> membranes were found. Other studies reported a higher critical flux for patterned UF<sup>44,55</sup> and TFC<sup>94,95</sup> membranes during filtration of model particles. Higher critical fluxes were reported for membrane patterns in an orientation perpendicular to the flow direction compared to patterns parallel to the flow direction.<sup>44</sup>

Furthermore, the influence of the particle-to-pattern size ratio was investigated. Jang et al. claimed that the fouling propensity of UF membranes in crossflow filtration is the lowest when the particle-to-pattern size ratio is three;<sup>93</sup> other studies confirmed these findings for particles substantially smaller than the pattern size.<sup>20,91</sup> In addition to experiments, modeling studies on the impact of surface patterning on particulate fouling propensity have been performed; these results are reviewed in Section 4.3.

Overall, crossflow filtration experiments with model particle foulants demonstrated that membrane surface patterns can reduce particulate fouling across various particle sizes,<sup>93</sup> pattern sizes,<sup>20</sup> and crossflow velocities.<sup>20</sup> However, further research is needed to investigate particulate fouling propensity in industry-relevant membrane configurations, such as spacer-filled channels.

**3.5. Effects of Surface Patterning on Biofouling Propensity and Potential Methodology Improvements.**

The effects of surface patterning on biofouling propensity have been extensively studied in previous studies, reaching from material-scale investigations<sup>35,54,72</sup> to engineering crossflow filtration tests.<sup>31,34,66</sup> On a material scale, the inherent capacity of surface patterned TFC and UF membranes to reduce the attachment of model microorganisms (e.g., *E. coli*, *S. epidermis*) under static conditions was investigated. Membrane coupons, each a few hundred square millimeters, were immersed for 24 h in a bacteria suspension; SEM micrographs showed reduced microorganism attachment on the patterned membranes.<sup>54</sup> CLSM analysis of static biofouling tests in drip-flow reactors revealed similar findings.<sup>34–36</sup> This antibiofouling propensity in static and drip-flow conditions was attributed to size exclusion effects.<sup>72</sup>

Antibiofouling properties of surface-patterned membranes were also tested under dynamic conditions. Short-term (i.e., up to 24 h) crossflow tests with permeation were conducted using suspensions of model foulants<sup>30,34,36,53,68</sup> or real feed waters.<sup>31,96</sup> These tests reported reduced flux decline for patterned MF membranes during filtration of baker's yeast that was attributed to a larger permeation area.<sup>53</sup> Additionally, a lower fouling rate of patterned MF<sup>68</sup> and TFC<sup>30,34,35</sup> membranes was observed during the filtration of *P. aeruginosa* suspensions. Choi et al. also reported that increasing the angle of Sharklet patterns from an orientation parallel to the flow to an orientation perpendicular to the flow reduces the flux decline during the filtration of *P. aeruginosa* suspension.<sup>97</sup> This enhanced antifouling performance was explained by a higher shear stress on the apexes of the pattern<sup>30,68</sup> and secondary flow structures created by the 3D surface patterns.<sup>34,35</sup> For surface patterns at the nanometer scale, size exclusion of bacteria model foulants was suggested as an additional mechanism of action.<sup>30</sup> Short-term crossflow filtration tests using real feed waters (i.e., MBR mixed liquor and activated sludge<sup>31,96</sup>) also demonstrated a higher antibiofouling propensity for patterned MF membranes, which was again attributed to higher shear stress on pattern apexes.<sup>31,96</sup> The multitude of suggested mechanisms of action indicates that the underlying processes of the antibiofouling behavior of surface-patterned MF/UF and TFC membranes are not yet entirely understood. A detailed discussion of these mechanisms of action is presented in Section 5.

The improved resistance of topographically patterned membranes to initial bacterial adhesion has been well-documented in both static conditions and short-term crossflow filtration (up to 24 h). However, continuous commercial applications of patterned membranes requires testing their resistance to biofilm growth—the main cause of biofouling in full-scale membrane-based water treatment systems—through either long-term filtration tests or accelerated biofouling tests employing real feedwater.<sup>98</sup> Wang et al. tested the crossflow filtration performance of a surface-patterned polyethylene-supported nanofiltration (NF) membrane compared to conventional flat-sheet TFC membranes.<sup>66</sup> Using NF concentrate as a feed, they reported a lower increase of TMP (an important indicator for biofouling in engineering practice) after 10 days of operation. In another study, patterned TFC membranes exhibited a lower flux decline rate compared to its flat counterpart in filtration tests using real seawater;<sup>34</sup> however, after 15 days of operation, there were no substantial differences between the fluxes of both membranes. This suggests that surface-patterned membranes have the potential



to initially reduce and delay biofouling, but as expected not completely prevent it.<sup>34</sup>

This discrepancy between antibiofouling performance of surface-patterned MF/UF and TFC membranes in short-term versus long-term filtration tests underlines that further research is needed to understand the impacts of surface patterning on membrane resistance to biofilm growth. Specifically, long-term filtration tests using real feed waters and operating conditions close to commercial applications should be conducted. This implies using flat-sheet crossflow cells with larger membrane coupon areas (several thousand square millimeters)<sup>66</sup> or lab-scale SWM. Besides, most biofouling studies on surface-patterned membranes have relied on flux measurements to evaluate membrane performance.<sup>34,35,53</sup> However, in future research, these studies should be complemented by measurements of typical parameters used to monitor biofouling in engineering practice, e.g., FCPD<sup>99</sup> and TMP.<sup>66</sup>

Regarding further analysis methods beyond the suggested parameters, CLSM<sup>34–36</sup> and SEM<sup>54</sup> have been employed to visualize and analyze the spatial and temporal development of biofouling, contributing to a better understanding of biofouling processes. However, these microscopy methods can be applied only after termination of a filtration test during membrane autopsy. Therefore, they should be supplemented by *in situ* real-time and nondestructive analytical methods. For flat-sheet test cells with small membrane surface areas (a few thousand square millimeters), optical coherence tomography (OCT)<sup>94</sup> and direct observation by optical microscopes or camera imaging<sup>100</sup> have been reported, whereas nuclear magnetic resonance (NMR) spectroscopy has been shown to be a suitable tool for biofouling monitoring in SWM.<sup>101,102</sup>

#### 4. CRITICAL ASSESSMENT OF THEORETICAL AND NUMERICAL METHODS FOR UNDERSTANDING THE EFFECTS OF SURFACE PATTERNING ON HYDRODYNAMICS AND MEMBRANE PERFORMANCE

**4.1. Particle Deposition on Topographically Heterogeneous Surfaces.** The interaction energy of colloidal sphere rigid particles on topographically heterogeneous surfaces, such as surface-patterned membranes, was simulated using mathematical models based on the Derjaguin–Landau–Verwey–Overbeek (DLVO) theory.<sup>103</sup> The DLVO theory estimates the total interaction energy between two surfaces as the sum of electrostatic double-layer and van der Waals interactions. Martines et al. calculated interaction energies between microsphere particles and patterned surfaces with nanostructures of various shapes and dimensions.<sup>104</sup> They observed that nanoprotusions and nanopillars can enhance particle adhesion, especially with reduced pillar dimensions. In contrast, nanopits caused less significant changes in interaction energy but were simulated to increase the energy barrier at lower particle concentration, thereby impeding particle deposition. Another study found that inducing nanotopography in the form of an array of cylindrical nanopillars can decrease the potential energy barrier for unfavorable surfaces.<sup>105</sup>

For the validation of DLVO calculations, the AFM force–distance curve method was utilized to examine the particle deposition behavior on rough membrane surfaces. This method, developed by Ducker et al.,<sup>106</sup> combines AFM and the colloid-probe technique. For instance, the potential energy

barrier for the deposition of silica spherical microparticles on a rough membrane surface was found to be lower than on a smoother corresponding surface.<sup>85,86</sup> Additionally, the magnitude of electrical double-layer repulsion on a rough membrane surface was reduced at the protruding apexes.<sup>107</sup> The adhesion of the colloid probe was lower at the roughness apexes than that in the valleys. Consequently, the deviation in the interaction energy between foulant particles and the membrane surface was strongly correlated to the topography of the membrane surface.<sup>108–110</sup>

**4.2. Hydrodynamic CFD Models to Characterize Flow Atop Surface-Patterned Membranes.** CFD modeling has been employed to study the flow characteristics in the direct vicinity of surface-patterned water separation membranes. These models are used to numerically estimate certain physical quantities (e.g., velocity field and shear stresses), which usually cannot, or only with considerable effort, be measured directly through bench-scale experiments. These quantities are crucial for understanding and the establishment of mechanisms of action. Most CFD models of surface-patterned membranes use continuum models of laminar, steady-state, incompressible Newtonian flow that are based on the Navier–Stokes equations.<sup>20,34,96</sup> However, models employing the Lattice-Boltzmann method,<sup>37</sup> molecular dynamics,<sup>91,92,111</sup> or turbulent flow models<sup>112</sup> are also present in the literature.

CFD studies of surface-patterned membranes typically comprised a hydrodynamic model to examine velocity fields, streamline plots, and shear stress distributions. The modeled flow conditions (e.g., crossflow velocity, flow rate, pressure, and Reynolds number) were derived from parallel bench-scale experiments.<sup>20,30,34,35,91,95</sup> To date, the vast majority of CFD studies on surface-patterned membranes modeled patterns using ideal geometric shapes at nanometer,<sup>93,95</sup> micrometer,<sup>34,37,92</sup> and millimeter<sup>113</sup> scales; examples include triangles<sup>20</sup> or half-circles<sup>93</sup> in 2D models, and prisms<sup>34</sup> or cylinders<sup>30</sup> in 3D models. However, SEM analysis revealed that real membrane surface patterns exhibited geometric irregularities in both shape and scale.<sup>23,30,34</sup> As a result, the ideal geometric shapes often used in CFD modeling cannot reliably account for these membranes. Figure 2 presents an overview of the limitations of current CFD modeling of surface-patterned membranes and recommendations for improving their accuracy and outputs.

To the best of our knowledge, only one CFD study has accounted for these geometric irregularities by modeling membrane surface patterns based on optical microscopy images and SEM micrographs.<sup>114</sup> The modeled flow fields over these irregularly shaped membrane surface patterns showed that local geometric irregularities could create highly localized, irregularly shaped flow disturbances and vortices.<sup>114</sup> This contrasts with modeling studies that use idealized triangular or rectangular surface pattern shapes, which showed repetitive, regular flow structures and vortices.<sup>6,115</sup> These findings highlight that CFD modeling outputs depend significantly on the accuracy of the modeled geometries.

Therefore, dedicated studies that critically examine the impact of geometric accuracy on the modeling outputs are needed. These studies should investigate key modeling parameters, including velocity fields, shear stress distribution, feed channel pressure drop, and membrane flux (if the membrane is to be modeled as a permeable surface) for different levels of geometric accuracy. Additionally, numerical results obtained for different levels of geometric accuracy

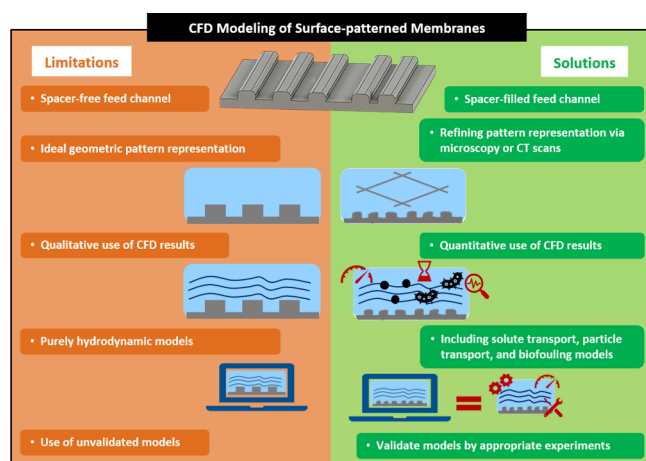


**Figure 2.** An overview of the limitations of current CFD modeling of surface-patterned membranes and recommendations for improving their accuracy and outputs.

should be properly validated by comparison with experimental data. Relevant work has recently been conducted in a closely related research area, i.e., the refinement of modeled feed spacer geometries.<sup>89,116</sup> In this work, refining feed spacer geometry from regular cylindrical filaments to X-ray computer tomography (CT) scan-derived geometries has showed close agreement between CFD modeling and experimental results for pressure drop and particle deposition.<sup>89</sup>

Another critical aspect in the CFD modeling of flow around membrane surface patterns is the geometry of the fluid domain. To reduce the computational effort, fluid domains in studies reported in the peer-reviewed literature are typically limited to a few pattern features, i.e., substantially smaller than the size of membrane coupons used in performance experiments (e.g., 800 mm<sup>2</sup> in performance experiments vs approximately 0.005 mm<sup>2</sup> in CFD modeling<sup>34</sup>). In a fluid domain with such reduced dimension (length and width), fully developed flow around a few pattern features without entrance, exit, or lateral wall effects can be accurately modeled by periodic boundary conditions.<sup>34,35</sup>

Regarding the fluid domain height, some studies considered the full height of the feed-retentate channel from crossflow membrane cells (based on parallel bench-scale experiments) and applied a no-slip condition to the upper domain boundary.<sup>92,117</sup> Others used a fraction of the full feed channel height as domain height and applied a fixed velocity (based on the fully developed laminar flow profile for the full channel height) as a moving wall condition to the upper domain boundary.<sup>6,37,91,117</sup> In both scenarios, a fully developed laminar flow profile for a spacer-free feed-retentate channel is assumed.<sup>6</sup> However, in commercially applied membrane configurations (e.g., SWM), the feed-retentate channels are equipped with feed spacers that disturb the fully developed laminar flow profile and dominate channel geometry and flow characteristics.<sup>89</sup> Feed spacers are traditionally used to allow intermembrane spacing, promote fluid mixing, enhance mass transfer, and reduce concentration polarization.<sup>89</sup> To approach practical application conditions of TFC membranes in SWM, assemblies of feed spacers and surface-patterned membranes should be investigated in future CFD modeling with a focus on studying the possible synergistic or interference effects on hydrodynamic flow conditions.

Qualitative results (e.g., velocity fields and vortices in the valleys) of hydrodynamic modeling studies have provided valuable insights into the flow characteristics in the direct vicinity of surface-patterned membranes. When combined with quantitative results from biofouling<sup>34,35</sup> or particle fouling experiments,<sup>20,95</sup> these qualitative CFD results have effectively contributed to propose mechanisms of action explaining the enhanced performance of surface-patterned membranes.<sup>34,93,94</sup> However, the role of hydrodynamics in the pattern valleys for the antifouling propensity of surface-patterned membranes is not yet fully understood (see Section 5 for details on action mechanisms). Therefore, future research should focus on the quantitative analysis of modeling results, e.g., investigating the spatial direction of the vortex and vortex velocity magnitudes.<sup>6</sup>

**4.3. Solute and Particle Transport CFD Models.** In addition to hydrodynamic models, solute transport models have been developed to investigate the effects of membrane surface-patterning on concentration polarization.<sup>6,62,118,119</sup> Mazinani et al. found a reduced concentration polarization for the flow over surface-patterned membranes with a 3D wavy pattern, attributing this to higher shear stress on the pattern apices.<sup>62</sup> Similar results were reported for prism- and half-cylinder-shaped surface-patterned membranes, installed perpendicular relative to the feed flow direction, which were explained by the creation of vortices in the pattern valleys that reduce the accumulation of solutes.<sup>120</sup> Additionally, Park et al. reported reduced concentration polarization for herringbone patterns and attributed their findings to substantially higher fluid mixing due to the presence of the patterns.<sup>119</sup> Conversely, Zhou et al. modeled flow over various pattern shapes (cuboids, prisms, pillars, etc.) and sizes (0.0625–256 μm pattern height), reporting an increased concentration polarization due to an increase of the boundary layer thickness that decreases the solute mass transfer away from the membrane surface.<sup>6</sup> These findings were supported by Chauhan et al.<sup>118</sup> Additionally, Zhou et al. stated that the velocity magnitudes of the observed vortices in the pattern valley regions are too low for effective foulant transport and subsequently discarded the creation of vortices in the valley regions as an antifouling mechanism.<sup>6</sup> Shang et al. attributed similar results to a larger PWP due to the enhanced active surface area of patterned membranes.<sup>117</sup> Further research is needed to thoroughly understand the effects of surface-patterning on concentration polarization and the underlying mechanisms of action.

Particle transport and deposition models have also been studied. These results showed stronger particle deposition in the pattern valleys than on the apices, which was consistent with bench-scale particle fouling experiments.<sup>91,92,113</sup> These findings were explained by higher shear stress on the pattern apices and stronger permeation drag in the pattern valleys.<sup>92</sup> Additionally, larger crossflow velocities were found to reduce particle deposition in both particle transport models and parallel particle fouling experiments, due to transport by the bulk flow<sup>91,113</sup> as well as the increased lift and drag forces on the particles.<sup>94</sup>

Overall, investigating solute and particle transport and deposition models has improved the general understanding of particle fouling and concentration polarization processes on surface-patterned membranes. Therefore, future research should more frequently complement hydrodynamic models with such solute and particle transport models. Additionally, biomass attachment and growth models should be incorporated into the numerical models of surface-patterned

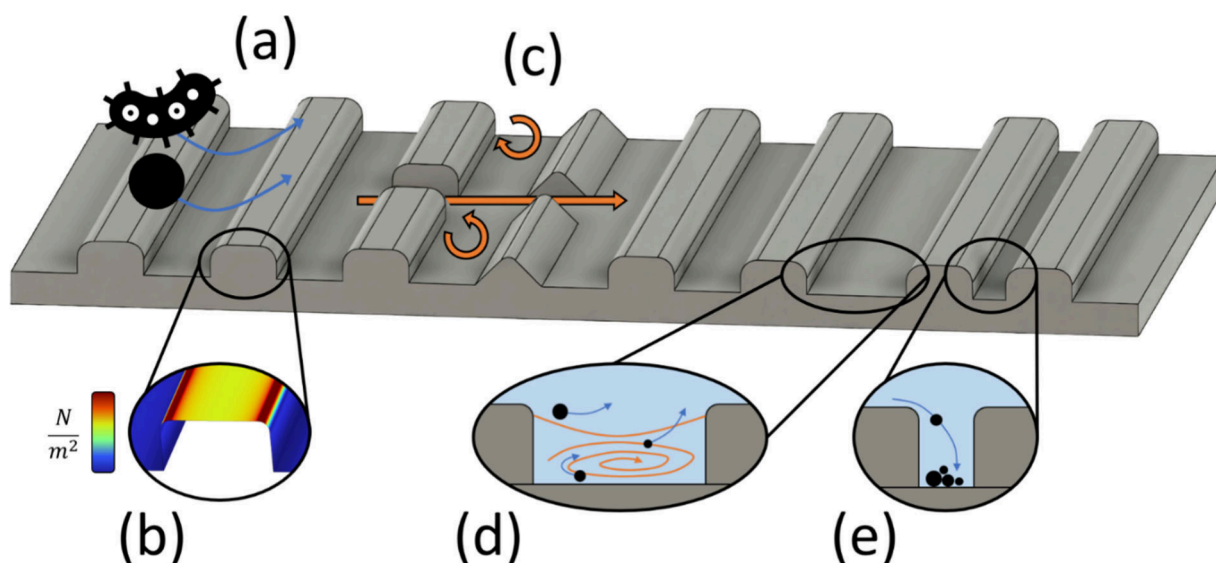


**Figure 3.** Proposed mechanisms of action in the literature: (a) size exclusion; (b) shear stress on pattern apices; (c) secondary flow structures; (d) vortex-induced shielding effect; (e) foulant deposition in stagnant fluid conditions. In this scheme, the surface patterns are perpendicular to the feed flow direction.

membranes in order to gain a better and deeper understanding of biofouling processes. In a related context, a mathematical model of biofouling on feed spacers enabled the investigation of the effect of feed spacer thickness and flow rate on biomass accumulation.<sup>121</sup> The numerical results of the FCPD increase due to biofouling were in satisfactory agreement with the experimental data, demonstrating the adequacy of numerical biofouling models while also highlighting potential areas for improvement.

By numerical simulation of these processes (solute and particle transport as well as biomass attachment and growth), comprehensive CFD models can better approximate the complex fouling conditions that prevail in membrane filtration of real feed waters. However, a crucial step in the use of numerical models is validation using experimental results. It is recommended that different numerical models should be validated against experimental data of the same physical phenomena, e.g., validating hydrodynamic models by PIV measurements<sup>86</sup> and solute transport models by salt retention or scaling experiments. Particle transport models should be validated with the mass deposition and surface coverage data from particle fouling experiments and biofouling models by FCPD or surface coverage data from biofouling experiments. Once validated with experimental results, numerical models can enable the cost-effective optimization of membrane surface pattern geometry toward an improved membrane performance.<sup>112,122</sup>

## 5. MECHANISMS OF ACTION INTERPRETING THE EFFECTS OF SURFACE PATTERNING ON MEMBRANE PERFORMANCE

Several mechanisms have been proposed to explain how membrane surface patterning influences both hydrodynamics and particles and foulants, ultimately affecting membrane fouling propensity. These mechanisms of action have been derived from bench-scale experiments and CFD modeling considering spacer-free feed-retentate channels. However, their applicability is somewhat limited as they do not account for or reliably predict the performance of surface-patterned mem-

branes in spacer-filled channels. Moreover, the alignment of surface structures relative to the feed flow direction in the feed-retentate channel was found to substantially influence the flow characteristics and particle deposition mechanisms. This has been demonstrated in bench-scale experiments,<sup>46,55,123–125</sup> modeling studies,<sup>6,29,80,124,125</sup> and a flow characterization study.<sup>86</sup>

To date, five general mechanistic effects of membrane surface patterning have been proposed in the literature to explain the improved performance of surface-patterned membranes in spacer-free channels, cf. Figure 3. These effects were reported for both dense and porous surface-patterned membranes when aligned perpendicular to the feed flow direction. Here, these mechanisms are thoroughly evaluated.

**5.1. Size Exclusion Mechanism.** Size exclusion is a critical yet straightforward mechanism<sup>30,72,126</sup> (see Figure 3 (a)). Surface structures that are smaller than the foulants (particles and microorganisms alike) can block the access of these foulants to the membrane surface, preventing accumulation in the pattern valley regions. For instance, studies have shown that bacteria with sizes larger than membrane surface micro- and nanostructures were unable to enter the pattern valleys, reducing bacterial adhesion.<sup>30,72,126</sup> Additionally, colloidal fouling experiments indicate that the size exclusion effect is most effective when the particle/pattern size ratio is approximately three.<sup>93</sup> However, this mechanism is not effective for foulants substantially smaller<sup>30,37,93</sup> or larger<sup>93</sup> than the pattern features.

**5.2. Shear Stress on the Pattern Apexes.** Another mechanistic effect proposed to explain the low fouling propensity of surface-patterned membranes is the high shear stress on the pattern apices (Figure 3 (b)). Many studies on colloidal fouling<sup>20,91–93</sup> and biofouling<sup>31,34,68,96</sup> have observed that foulants tend to deposit preferentially in the pattern valleys rather than on the apices. Hydrodynamic CFD models confirm that shear stress is substantially higher around pattern apices (especially on pattern apex edges) than in the valleys.<sup>20,30,35,93</sup> It is thus well accepted that the protruding

geometry of pattern apexes can lead to higher local shear stress and less foulant deposition.

**5.3. Generation of Secondary Flow Structures.** The introduction of the Sharklet pattern<sup>34</sup> raised questions concerning additional mechanisms contributing to the performance of discontinuous three-dimensional patterns. While size exclusion and high shear stress on apexes are demonstrated and accepted to a good degree, the creation of secondary flow structures has been proposed as a major mechanistic effect minimizing the biofoulant deposition<sup>34–36</sup> (see Figure 3 (c)). Hydrodynamic CFD modeling revealed that up- and downward flow structures perpendicular to the bulk flow (so-called *secondary* flow structures) are generated within the discontinuous pattern valleys.<sup>34,35</sup> Besides, comparatively high velocity in the bulk flow direction and low bacterial adhesion coincide in the spacing between unit blocks of the discontinuous patterns.<sup>34</sup> These flow structures are substantially different from typical flow structures in continuous patterns. Consequently, the enhanced antifouling propensity of discontinuous patterns, especially of the Sharklet pattern, is attributed to the secondary flow structures.

**5.4. Vortex-Induced Shield Effects.** The vortex-induced shield effect mechanism concerns the hydrodynamic conditions in the pattern valley regions. Hydrodynamic CFD models have shown the formation of vortices in the pattern valleys, similar to lid-driven flow in a cavity.<sup>6</sup> These vortices coincide with an improved antifouling performance in supplement bench-scale experiments.<sup>20,94,120</sup> Hence, it is argued that the flow separation between bulk flow and vortex flow prevents foulants from entering the pattern valley regions, creating the so-called antifouling “vortex-induced shield effect”<sup>34,35</sup> (see Figure 3 (d)). Additionally, these vortices are suggested to prevent foulant accumulation and deposition on the membrane surface<sup>94,120</sup> and allow foulants to re-enter the bulk flow.<sup>20</sup>

However, some studies have reported that the velocity magnitudes of these vortices are too low to transport foulants away from the membrane, indicating that further investigation is needed. Several studies reported the observation of vortices in the pattern valleys,<sup>20,94,120</sup> whereas only few studies performed a quantitative analysis of these vortices and their ability to transport foulants by hydrodynamic forces. Zhou et al. suggested that the velocity magnitudes of vortices in the pattern valleys were too low to transport foulants away from the membrane.<sup>6</sup> These low vortex velocity magnitudes in the pattern valleys can be observed in many hydrodynamic CFD models.<sup>20,35,57,94,120</sup> Besides, Yoo et al. revealed that the lift forces on foulant particles are substantially lower in the vortex-filled valleys of the 3D discontinuous Sharklet<sup>37</sup> pattern than in the spacings between unit blocks. Accordingly, these results emphasize that further investigation of the “vortex-induced shield effect” is required.

**5.5. Foulant Deposition in Stagnant Fluid Conditions.** Reducing the crossflow velocity or the width of pattern valley regions can reduce the “vortex-induced shield effect”<sup>35</sup> (see Figure 3 (d) and (e)). If foulants enter these pattern valleys with a reduced or absent “vortex-induced shield effect”, they encounter stagnant fluid conditions that can facilitate their deposition (Figure 3 (e)). Many studies have consistently observed higher foulants (particles) deposition in pattern valleys than on pattern apexes during crossflow filtration of colloid suspensions<sup>91–93</sup> and real waters<sup>31,96</sup> using surface-patterned membranes. These results can be explained by

stagnant fluid conditions in the pattern valleys that are characterized by low velocity<sup>92,96</sup> and low shear stress.<sup>92,93</sup> These conditions are argued to create an ideal environment for foulant aggregation<sup>96</sup> and transport to the membrane surface by permeation drag<sup>117</sup> and membrane-foulant attractive forces.<sup>92</sup>

The experimental and modeling results that motivated the two last mechanisms suggest that hydrodynamic conditions in the pattern valleys can play a crucial role to understand the (anti) fouling properties of surface-patterned membranes. Future research should focus on the quantitative analysis of these hydrodynamic conditions, for instance, by investigating the vortex velocity magnitudes,<sup>6,113</sup> the role of flow pulses,<sup>127</sup> hydrodynamic forces acting on foulant particles,<sup>37,93,94,128</sup> as well as local magnitudes of shear stress, flux, and concentration polarization modulus on pattern apexes and in pattern valleys.<sup>118,119</sup> These improved analysis tools will allow a more thorough investigation of the role of hydrodynamic conditions and vortices in pattern valleys on the antifouling properties of surface-patterned membranes.

## 6. IMPACT OF MEMBRANE SURFACE-PATTERNING ON HYDRODYNAMIC CLEANING EFFICIENCY

While membrane surface-patterning can reduce and/or delay membrane fouling under certain operating conditions, it cannot entirely prevent membrane fouling during long-term operation.<sup>34,66</sup> Therefore, in this section, we discuss experimental studies that have examined the cleaning efficiency of surface-patterned water separation membranes and the effects of surface-patterning on postfouling hydrodynamic cleaning.

For various membrane fouling types (e.g., organic fouling and biofouling), the flux recovery ratio (FRR) serves as a reliable parameter to effectively assess the overall fouling resistance of a membrane. FRR is defined as the ratio of PWP for a cleaned membrane (after fouling) to that of a virgin membrane (before testing).<sup>47</sup> Several studies in the literature compared FRR values of surface-patterned membranes vs flat membranes during different filtration (fouling) tests using model protein solution (bovine serum albumin),<sup>25,47</sup> model bacteria solution (*E. coli*),<sup>58,72</sup> and aerobic MBR mixed liquor.<sup>54</sup> Surface-patterned membranes with different pattern designs were tested in bench-scale experimental setups (dead-end stirred cells<sup>54,72</sup> vs crossflow cells<sup>25,47,58</sup>). Various membrane cleaning methods were used. For example, Maruf et al. as well as Rickman et al. cleaned fouled membranes *in situ* by forward flushing using deionized water in a crossflow cell, without applying pressure.<sup>25,47</sup> Ma et al. followed a similar approach using a dead-end stirred cell with an increased stirring rate,<sup>54</sup> whereas Yoo et al. performed *ex-situ* cleaning by rinsing fouled membranes in deionized water.<sup>58</sup> Across all these studies, surface-patterned membranes consistently showed improved FRR values compared to flat counterparts.<sup>25,47,54,58,72</sup> However, the extent of improvement varied, with some studies reporting significantly higher FRR values for patterned membranes,<sup>25,47,72</sup> while others observed minor differences.<sup>54,58</sup> Additionally, Maruf et al. found that CaSO<sub>4</sub> crystals deposited on surface-patterned TFC membranes during 24 h of stirred dead-end filtration experiments were easier to remove by rinsing compared to those on flat-sheet membranes.<sup>45</sup>

Other experimental studies have investigated the effects of surface-patterning on hydrodynamics near the membrane surface and foulants detachment. Various surface pattern

sizes,<sup>20</sup> operating conditions,<sup>20,96,129</sup> testing procedures.<sup>52,56</sup> were examined. For instance, Gohari et al. investigated how membrane orientation, relative to feed flow direction, affects foulant attachment and removal at a high flow rate (200 L/h, equivalent to a turbulent flow regime).<sup>129</sup> The perpendicular orientation of surface patterns relative to the feed flow direction was found to minimize protein attachment during filtration mode due to enhanced fluid mixing, while the parallel orientation was more effective during cleaning experiments (forward flushing) because of a stronger sweeping effect on foulants in the valley regions.

Recently, the enhanced cleaning properties of surface-patterned membranes have been combined with other antifouling approaches to improve fouling-release characteristics for water separation membranes. For instance, ElSherbiny et al. combined surface-patterning with hydrogel coating to promote the antifouling propensity of surface-patterned TFC membranes during sophisticated dead-end filtration of micro- and nanosilica particles.<sup>56</sup> In another study, Ilyas et al. demonstrated an improved cleaning efficiency for surface-patterned polyvinylidene difluoride membranes in wastewater filtration when vibration was introduced due to the improved hydrodynamics.<sup>52</sup>

Primary mechanistic effects (particularly, increased shear stress on pattern apices, formation of vortices in pattern valleys, and generation of secondary flow structures), which explain the effects of surface patterning on hydrodynamics and foulant deposition (cf. Section 5), can also explain the enhanced fouling-release features for surface-patterned membranes during hydraulic cleaning experiments. However, the dimensions of surface patterns (e.g., feature height, spacing) are also critical factors influencing foulant detachment. For example, Won et al. compared the deposition of 2  $\mu\text{m}$ -sized latex particles on small (25  $\mu\text{m}$  height) and large (400  $\mu\text{m}$  height) prism-shaped surface patterns at different Reynolds numbers.<sup>20</sup> At a lower Reynolds number ( $Re = 600$ ), small prism-shaped surface patterns showed lower particles deposition, whereas at a higher Reynolds number ( $Re = 1,600$ ), large patterns performed better. The impacts of pattern spacing on particle deposition were also examined.<sup>20</sup> Larger spacing (800  $\mu\text{m}$  and 1,200  $\mu\text{m}$ ) resulted in lower particle deposition compared to smaller spacing (400  $\mu\text{m}$ ), while more particle deposition was observed for spacing  $>1,200 \mu\text{m}$ .

In conclusion, topographical surface modification can enhance the fouling-resistant or fouling-releasing properties under certain conditions, leading to an improved membrane performance. However, further research is needed to explore these potential effects under industrial application relevant operating conditions (see Section 3.5), including long-term filtration experiments (with/without periodic hydrodynamic cleaning), operation using real feedwater, and application in spacer-filled channels.

**7. Future Challenges and Research Needs.** Based on our thorough and comprehensive assessment of the state-of-the-art, we present the following recommendations for advancing the current research toward full-scale application of surface-patterned water separation membranes and enhancing the understanding of the mechanisms behind their improved performance:

**7.1. Evaluation of Surface-Patterned TFC Membranes in Spacer-Filled Channels.** The state-of-the-art membrane configuration in commercial-scale applications, SWMs, consists of TFC membranes, feed spacers, and permeate spacers.

Therefore, it is essential for both experimental and numerical studies to examine the performance of surface-patterned membranes in combination with typical feed spacers. This evaluation is crucial to reliably assess the applicability of newly developed surface-patterned membranes for full-scale applications.

**7.2. Testing of Surface-Patterned Membranes in Combination with Feed Spacers Will Introduce a New Design Criterion for Membrane Patterns.** Due to the different hydrodynamic effects induced by surface-patterned membranes and feed spacers, the synergistic effects of both structures should be adequately investigated and better understood to effectively identify scenarios where their combination may have an added value. Furthermore, membrane surface patterns can be specifically designed to address certain flaws in the feed spacers.

**7.3. Upscaling Roll-to-Roll (R2R) Patterning Methods.** R2R thermal embossing methods using hard stamps have demonstrated the potential for producing industrial-sized surface-patterned porous and dense membranes. However, patterning conditions must robustly achieve the desired pattern depths/heights while preventing excessive compaction of membrane layers and cracking of the membrane polymer, in addition to maintaining the membrane physical characteristics (e.g., porosity).

**7.4. Development of Alternative Fabrication Approaches for Complex Membrane Patterns.** Replicating complex 3D pattern structures onto dense TFC membranes may require further development of more two-step synthesis approaches, in which the surface pattern fidelity can be individually enhanced, while the dense layer characteristics, including layer thickness along the complex surface structures and perm-selectivity, can be effectively optimized.

**7.5. Development of Standardized Characterization Methods.** To effectively understand the impact of surface-patterning on performance-influencing structural and physicochemical properties, it is essential to establish standardized characterization methods for surface-patterned membranes, particularly for TFC membranes. As discussed in Section 2.3, there is a knowledge gap regarding the effect of surface-patterning on critical physicochemical properties, such as membrane surface charge and affinity. Furthermore, standardized methods relevant to surface-patterned membranes should be developed. Both pattern height fidelity and the increase of membrane active surface area are key parameters that are frequently being used in the literature; however, they have not yet been standardized.

**7.6. Establishing Representative, Standardized Membrane Performance Tests.** Most performance tests for surface-patterned membranes were conducted in dead-end mode under constant pressure, without feed spacers, and using bench-scale setups. Subsequently, the relevance of their results to practical membrane filtration scenarios may be questionable. Therefore, standardized testing methods that closely simulate industrial-scale operating conditions are needed to evaluate key performance parameters such as PWP, salt retention, and concentration polarization. Additionally, these tests should be expanded to include common fouling types encountered in real-world applications, including scaling and biofouling.

**7.7. Intensifying Research on (Upscaling) Fabrication of Surface-Patterned Dense Membranes Using Unconventional Interfacial Polymerization Methods.** Recent studies highlight the potential of unconventional interfacial polymer-

ization methods, such as layered interfacial polymerization and spin-drying assisted interfacial polymerization, to fabricate uniform, conformal, and thin polyamide layers on patterned membrane supports with different surface patterns designs. Future research should also explore other methods, such as dual-layer slot coating and electrospray techniques, for their feasibility and effectivities. Moreover, upscaling these methods for industrial-sized membrane fabrication should be a key focus to facilitate practical, full-scale applications.

**7.8. Real-Time Hydrodynamic Measurements for the Flow near Surface-Patterned Membranes.** To date, flow hydrodynamics in the direct vicinity of surface-patterned membranes have largely been studied through CFD modeling, which may not accurately reflect real geometry and flow conditions. To develop a thorough understanding of hydrodynamics atop surface-patterned membranes, real-time fluid characterization experiments using noninvasive visualization techniques, such as PIV, are essential. PIV provides detailed, quantitative flow field data, allowing for analysis of fluid dynamics within pattern valleys and around apexes. This approach will be instrumental in validating CFD models and critically evaluating the primary mechanistic effects reported in the literature. It is also recommended to conduct these tests under operating conditions that simulate industrial-scale applications, which will help decouple the effects of surface-patterning from intrinsic membrane properties on overall membrane performance.

**7.9. Enhanced Antibiofouling Experiments Investigating Long-Term Effects, Adequately Equipped with Real-Time Analysis Tools.** Given the substantial impact of biofouling in commercial-scale membrane applications, it is crucial to intensify experimental studies on the long-term antibiofouling properties of surface-patterned membranes. This requires long-term filtration tests with real feed waters under conditions that closely simulate full-scale commercial applications and the use of flat-sheet crossflow cells with larger membrane coupons or lab-scale SWM. The antibiofouling performance should be assessed by online measurement of parameters used in engineering practice (e.g., FCPD and TMP) and complemented by real-time, nondestructive analytical tools (e.g., NMR).

**7.10. Intensifying Research on the Effect of Surface Patterning on Hydrodynamic Cleaning Efficiency.** Further research is needed to explore the potential fouling-resistant and fouling-releasing properties of surface-patterned membranes under industrial-scale relevant operating conditions, including long-term filtration experiments (with/without periodic *in situ* hydrodynamic cleaning), operation using real feed waters, and application in spacer-filled channels.

**7.11. Improved CFD Models of Flow in the Vicinity of Surface-Patterned Membranes.** The accuracy at which the geometry of real membrane surface patterns is represented in CFD modeling can impact the results computed. This impact should be critically assessed in dedicated studies investigating key modeling parameters for different levels of geometric accuracy (e.g., pattern geometries based on optical microscopy, SEM, or CT scans). Furthermore, quantitative analysis of hydrodynamic models should be intensified by investigating spatial vortex orientation, vortex velocity magnitudes, the role of flow pulses, and local magnitudes of shear stress and flux on pattern apexes and in pattern valleys.

**7.12. Integration of Solute and Particle Transport Models.** Numerical hydrodynamic models should be complemented

more frequently by solute transport, particle transport, and biofouling models to better simulate the complex fouling conditions encountered in the membrane filtration of real feed waters. These models must be validated against experimental data of the same physical phenomena. For instance, hydrodynamic models can be validated using PIV measurements, while particle transport models can be validated using mass deposition and surface coverage data from particle fouling experiments. Validated models should then be utilized to optimize the membrane pattern geometry, thereby enhancing the performance of surface-patterned membranes.

## AUTHOR INFORMATION

### Corresponding Authors

**Jörg E. Drewes** – Chair of Urban Water Systems Engineering, Technical University of Munich, 85748 Garching, Germany; [orcid.org/0000-0003-2520-7596](https://orcid.org/0000-0003-2520-7596); Email: [jdrewes@tum.de](mailto:jdrewes@tum.de)

**Ibrahim M. A. ElSherbiny** – Chair for Mechanical Process Engineering & Water Technology, University of Duisburg-Essen, 47057 Duisburg, Germany; [orcid.org/0000-0001-8885-450X](https://orcid.org/0000-0001-8885-450X); Email: [ibrahim.elsherbiny@uni-due.de](mailto:ibrahim.elsherbiny@uni-due.de)

### Authors

**Alexander Mitranescu** – Chair of Urban Water Systems Engineering, Technical University of Munich, 85748 Garching, Germany

**Maharshi Patel** – Chair for Mechanical Process Engineering & Water Technology, University of Duisburg-Essen, 47057 Duisburg, Germany

**Stefan Panglisch** – Chair for Mechanical Process Engineering & Water Technology, University of Duisburg-Essen, 47057 Duisburg, Germany; [orcid.org/0000-0001-6605-5010](https://orcid.org/0000-0001-6605-5010)

Complete contact information is available at:

<https://pubs.acs.org/10.1021/acsestwater.4c00779>

### Author Contributions

#A.M. and M.P. contributed equally to this work. CRediT: **Alexander Mitranescu** data curation, formal analysis, investigation, software, validation, visualization, writing - original draft; **Maharshi Patel** conceptualization, data curation, formal analysis, investigation, visualization, writing - original draft; **Stefan Panglisch** conceptualization, funding acquisition, project administration, resources, supervision, writing - review & editing; **Jörg E. Drewes** conceptualization, funding acquisition, project administration, resources, supervision, writing - review & editing; **Ibrahim M.A. ElSherbiny** conceptualization, data curation, investigation, project administration, resources, supervision, writing - review & editing.

### Notes

The authors declare no competing financial interest.

## ACKNOWLEDGMENTS

This study was funded by the German Research Foundation (DFG), award number 499318495.

## REFERENCES

- Çulfaz, P. Z.; Rolevink, E.; van Rijn, C.; Lammertink, R. G.; Wessling, M. Microstructured hollow fibers for ultrafiltration. *Journal of membrane science* **2010**, *347* (1–2), 32–41.
- Çulfaz, P. Z.; Buetehorn, S.; Utiu, L.; Kueppers, M.; Bluemich, B.; Melin, T.; Wessling, M.; Lammertink, R. G. Fouling behavior of microstructured hollow fiber membranes in dead-end filtrations:

- critical flux determination and NMR imaging of particle deposition. *Langmuir* **2011**, *27* (5), 1643–1652.
- (3) Ehrfeld, W.; Einhaus, R.; Münchmeyer, D.; Strathmann, H. Microfabrication of membranes with extreme porosity and uniform pore size. *J. Membr. Sci.* **1988**, *36*, 67–77.
- (4) Okada, T.; Matsuura, T. Pattern formation on the surface of cellulose membranes prepared by phase inversion technique. *Industrial & engineering chemistry research* **1988**, *27* (7), 1335–1338.
- (5) ElSherbiny, I. M. A. Novel micro- and nano-patterned water desalination membranes. Universität Duisburg-Essen, 2017.
- (6) Zhou, Z.; Ling, B.; Battiatto, I.; Husson, S. M.; Ladner, D. A. Concentration polarization over reverse osmosis membranes with engineered surface features. *Journal of membrane science* **2021**, *617*, 118199.
- (7) Ward, L. M.; Fickling, B. G.; Weinman, S. T. Effect of nanopatterning on concentration polarization during nanofiltration. *Membranes* **2021**, *11* (12), 961.
- (8) Durand, H.; Whiteley, A.; Mailley, P.; Nonglaton, G. Combining Topography and Chemistry to Produce Antibiofouling Surfaces: A Review. *ACS Applied Bio Materials* **2022**, *5* (10), 4718–4740.
- (9) Choudhury, R. R.; Gohil, J. M.; Mohanty, S.; Nayak, S. K. Antifouling, fouling release and antimicrobial materials for surface modification of reverse osmosis and nanofiltration membranes. *Journal of Materials Chemistry A* **2018**, *6* (2), 313–333.
- (10) Ilyas, A.; Vankelecom, I. F. J. Designing sustainable membrane-based water treatment via fouling control through membrane interface engineering and process developments. *Adv. Colloid Interface Sci.* **2023**, *312*, 102834.
- (11) Zhang, X.; Ma, J.; Zheng, J.; Dai, R.; Wang, X.; Wang, Z. Recent advances in nature-inspired antifouling membranes for water purification. *Chemical Engineering Journal* **2022**, *432*, 134425.
- (12) Heinz, O.; Aghajani, M.; Greenberg, A. R.; Ding, Y. Surface-patterning of polymeric membranes: fabrication and performance. *Current opinion in chemical engineering* **2018**, *20*, 1–12.
- (13) Wang, Q.; Lin, W.; Chou, S.; Dai, P.; Huang, X. Patterned membranes for improving hydrodynamic properties and mitigating membrane fouling in water treatment: A review. *Water Res.* **2023**, *236*, 119943.
- (14) Aung, H. H.; Patel, R. Recent Progress in Patterned Membranes for Membrane-Based Separation Process. *Membrane Journal* **2021**, *31* (3), 170–183.
- (15) Ibrahim, Y.; Hilal, N. A Critical Assessment of Surface-Patterned Membranes and Their Role in Advancing Membrane Technologies. *ACS ES&T Water* **2023**, *3* (12), 3807–3834.
- (16) Barambu, N. U.; Bilad, M. R.; Wibisono, Y.; Jaafar, J.; Mahlia, T. M. I.; Khan, A. L. Membrane surface patterning as a fouling mitigation strategy in liquid filtration: A review. *Polymers* **2019**, *11* (10), 1687.
- (17) Ding, Y.; Maruf, S.; Aghajani, M.; Greenberg, A. R. Surface patterning of polymeric membranes and its effect on antifouling characteristics. *Sep. Sci. Technol.* **2017**, *52* (2), 240–257.
- (18) Zare, S.; Kargari, A. State-of-the-art surface patterned membranes fabrication and applications: A review of the current status and future directions. *Chem. Eng. Res. Des.* **2023**, *196*, 495–525.
- (19) Chauhan, D.; Nagar, P. K.; Pandey, K.; Awasthi, K.; Pandey, H. Simulations of Physically Surface-Patterned Membranes for Water Treatment: Recent Advances. *Separation & Purification Reviews* **2024**, *53* (3), 250–275.
- (20) Won, Y.-J.; Jung, S.-Y.; Jang, J.-H.; Lee, J.-W.; Chae, H.-R.; Choi, D.-C.; Hyun Ahn, K.; Lee, C.-H.; Park, P.-K. Correlation of membrane fouling with topography of patterned membranes for water treatment. *Journal of Membrane Science* **2016**, *498*, 14–19.
- (21) Ilyas, A.; Mertens, M.; Oyaert, S.; Vankelecom, I. F. J. Synthesis of patterned PVDF ultrafiltration membranes: Spray-modified non-solvent induced phase separation. *Journal of membrane science* **2020**, *612*, 118383.
- (22) Marbelia, L.; Ilyas, A.; Dierick, M.; Qian, J.; Achille, C.; Ameloot, R.; Vankelecom, I. F. J. Preparation of patterned flat-sheet membranes using a modified phase inversion process and advanced casting knife construction techniques. *Journal of membrane science* **2020**, *597*, 117621.
- (23) Zhao, Z.; Ilyas, A.; Muylaert, K.; Vankelecom, I. F. J. Optimization of patterned polysulfone membranes for microalgae harvesting. *Bioresource technology* **2020**, *309*, 123367.
- (24) Maruf, S. Surface Patterning of Polymeric Separation Membranes and its Influence on the Filtration Performance. University of Colorado, 2014.
- (25) Rickman, M.; Maruf, S.; Kujundzic, E.; Davis, R. H.; Greenberg, A.; Ding, Y.; Pellegrino, J. Fractionation and flux decline studies of surface-patterned nanofiltration membranes using NaCl-glycerol-BSA solutions. *Journal of membrane science* **2017**, *527*, 102–110.
- (26) Weinman, S. T.; Husson, S. M. Influence of chemical coating combined with nanopatterning on alginate fouling during nanofiltration. *Journal of membrane science* **2016**, *513*, 146–154.
- (27) He, X.; Wang, T.; Li, Y.; Chen, J.; Li, J. Fabrication and characterization of micro-patterned PDMS composite membranes for enhanced ethanol recovery. *J. Membr. Sci.* **2018**, *563*, 447–459.
- (28) Choi, D.-C.; Jung, S.-Y.; Won, Y.-J.; Jang, J. H.; Lee, J.; Chae, H.-R.; Ahn, K. H.; Lee, S.; Park, P.-K.; Lee, C.-H. Three-dimensional hydraulic modeling of particle deposition on the patterned isopore membrane in crossflow microfiltration. *Journal of membrane science* **2015**, *492*, 156–163.
- (29) Choi, D.-C.; Jung, S.-Y.; Won, Y.-J.; Jang, J. H.; Lee, J.-W.; Chae, H.-R.; Lim, J.; Ahn, K. H.; Lee, S.; Kim, J.-H.; et al. Effect of Pattern Shape on the Initial Deposition of Particles in the Aqueous Phase on Patterned Membranes during Crossflow Filtration. *Environmental Science & Technology Letters* **2017**, *4* (2), 66–70.
- (30) Choi, W.; Chan, E. P.; Park, J.-H.; Ahn, W.-G.; Jung, H. W.; Hong, S.; Lee, J. S.; Han, J.-Y.; Park, S.; Ko, D.-H.; Lee, J.-H. Nanoscale pillar-enhanced tribological surfaces as antifouling membranes. *ACS Appl. Mater. Interfaces* **2016**, *8* (45), 31433–31441.
- (31) Won, Y.-J.; Lee, J.; Choi, D.-C.; Chae, H. R.; Kim, I.; Lee, C.-H.; Kim, I.-C. Preparation and application of patterned membranes for wastewater treatment. *Environ. Sci. Technol.* **2012**, *46* (20), 11021–11027.
- (32) Liu, Y.; Kodama, T.; Kojima, T.; Taniguchi, I.; Seto, H.; Miura, Y.; Hoshino, Y. Fine-tuning of the surface porosity of micropatterned polyethersulfone membranes prepared by phase separation micro-molding. *Polym. J.* **2020**, *52* (4), 397–403.
- (33) Lee, J.; Won, Y.-J.; Choi, D.-C.; Lee, S.; Park, P.-K.; Choo, K.-H.; Oh, H.-S.; Lee, C.-H. Micro-patterned membranes with enzymatic quorum quenching activity to control biofouling in an MBR for wastewater treatment. *J. Membr. Sci.* **2019**, *592*, 117365.
- (34) Choi, W.; Lee, C.; Lee, D.; Won, Y. J.; Lee, G. W.; Shin, M. G.; Chun, B.; Kim, T.-S.; Park, H.-D.; Jung, H. W.; Lee, J. S.; Lee, J.-H. Sharkskin-mimetic desalination membranes with ultralow biofouling. *Journal of Materials Chemistry A* **2018**, *6* (45), 23034–23045.
- (35) Choi, W.; Lee, C.; Yoo, C. H.; Shin, M. G.; Lee, G. W.; Kim, T.-S.; Jung, H. W.; Lee, J. S.; Lee, J.-H. Structural tailoring of sharkskin-mimetic patterned reverse osmosis membranes for optimizing biofouling resistance. *Journal of membrane science* **2020**, *595*, 117602.
- (36) Choi, W.; Shin, M. G.; Yoo, C. H.; Park, H.; Park, Y.-I.; Lee, J. S.; Lee, J.-H. Desalination membranes with ultralow biofouling via synergistic chemical and topological strategies. *Journal of membrane science* **2021**, *626*, 119212.
- (37) Yoo, C. H.; Lee, G. W.; Choi, W.; Shin, M. G.; Lee, C.; Shin, J. H.; Son, Y.; Chun, B.; Lee, J.-H.; Jung, H. W.; Lee, J. S. Identifying the colloidal fouling behavior on the sharkskin-mimetic surface: In-situ monitoring and lattice Boltzmann simulation. *Chemical Engineering Journal* **2021**, *405*, 126617.
- (38) Lee, C.; Lee, G. W.; Choi, W.; Yoo, C. H.; Chun, B.; Lee, J. S.; Lee, J.-H.; Jung, H. W. Pattern flow dynamics over rectangular Sharklet patterned membrane surfaces. *Appl. Surf. Sci.* **2020**, *514*, 145961.
- (39) Zhao, Z.; Muylaert, K.; Szymczyk, A.; Vankelecom, I. F. J. Harvesting microalgal biomass using negatively charged polysulfone

patterned membranes: Influence of pattern shapes and mechanism of fouling mitigation. *Water research* **2021**, *188*, 116530.

(40) Ilyas, A.; Mertens, M.; Oyaert, S.; Vankelecom, I. F. J. Anti-fouling behavior of micro-patterned PVDF membranes prepared via spray-assisted phase inversion: Influence of pattern shapes and flow configuration. *Sep. Purif. Technol.* **2021**, *259*, 118041.

(41) Ng, T. C. A.; Lyu, Z.; Wang, C.; Guo, S.; Poh, W.; Gu, Q.; Zhang, L.; Wang, J.; Ng, H. Y. Effect of surface-patterned topographies of ceramic membranes on the filtration of activated sludge and their interaction with different particle sizes. *J. Membr. Sci.* **2022**, *645*, 120125.

(42) Wardrip, N. C.; Dsouza, M.; Urgun-Demirtas, M.; Snyder, S. W.; Gilbert, J. A.; Arnusch, C. J. Printing-assisted surface modifications of patterned ultrafiltration membranes. *ACS Appl. Mater. Interfaces* **2016**, *8* (44), 30271–30280.

(43) Field, R. W.; Pearce, G. K. Critical, sustainable and threshold fluxes for membrane filtration with water industry applications. *Adv. Colloid Interface Sci.* **2011**, *164* (1–2), 38–44.

(44) Maruf, S. H.; Greenberg, A. R.; Pellegrino, J.; Ding, Y. Critical flux of surface-patterned ultrafiltration membranes during cross-flow filtration of colloidal particles. *Journal of membrane science* **2014**, *471*, 65–71.

(45) Maruf, S. H.; Greenberg, A. R.; Pellegrino, J.; Ding, Y. Fabrication and characterization of a surface-patterned thin film composite membrane. *Journal of membrane science* **2014**, *452*, 11–19.

(46) ElSherbiny, I. M. A.; Khalil, A. S. G.; Ulbricht, M. Surface micro-patterning as a promising platform towards novel polyamide thin-film composite membranes of superior performance. *Journal of membrane science* **2017**, *529*, 11–22.

(47) Maruf, S. H.; Rickman, M.; Wang, L.; Mersch IV, J.; Greenberg, A. R.; Pellegrino, J.; Ding, Y. Influence of sub-micron surface patterns on the deposition of model proteins during active filtration. *Journal of membrane science* **2013**, *444*, 420–428.

(48) Xie, M.; Luo, W.; Gray, S. R. Surface pattern by nanoimprint for membrane fouling mitigation: Design, performance and mechanisms. *Water Res.* **2017**, *124*, 238–243.

(49) Asad, A.; Sadrzadeh, M.; Sameoto, D. Direct Micropatterning of Phase Separation Membranes Using Hydrogel Soft Lithography. *Advanced Materials Technologies* **2019**, *4* (7). DOI: 10.1002/admt.201800384.

(50) Asad, A.; Aktij, S. A.; Karami, P.; Sameoto, D.; Sadrzadeh, M. Micropatterned thin-film composite poly (piperazine-amide) nanofiltration membranes for wastewater treatment. *ACS Applied Polymer Materials* **2021**, *3* (12), 6653–6665.

(51) Ilyas, A.; Yihdego Gebreyohannes, A.; Qian, J.; Reynaerts, D.; Kuhn, S.; Vankelecom, I. F. J. Micro-patterned membranes prepared via modified phase inversion: Effect of modified interface on water fluxes and organic fouling. *J. Colloid Interface Sci.* **2021**, *585*, 490–504.

(52) Ilyas, A.; Timmermans, L.; Vanierschot, M.; Smets, I.; Vankelecom, I. F. J. Micro-patterned PVDF membranes and magnetically induced membrane vibration system for efficient membrane bioreactor operation. *Journal of membrane science* **2022**, *662*, 120978.

(53) Gençal, Y.; Durmaz, E. N.; Çulfaz-Emecen, P. Z. Preparation of patterned microfiltration membranes and their performance in crossflow yeast filtration. *Journal of membrane science* **2015**, *476*, 224–233.

(54) Ma, Z.; Liang, S.; Xiao, K.; Wang, X.; Li, M.; Huang, X. Superhydrophilic polyvinylidene fluoride membrane with hierarchical surface structures fabricated via nanoimprint and nanoparticle grafting. *Journal of membrane science* **2020**, *612*, 118332.

(55) Maruf, S. H.; Wang, L.; Greenberg, A. R.; Pellegrino, J.; Ding, Y. Use of nanoimprinted surface patterns to mitigate colloidal deposition on ultrafiltration membranes. *Journal of membrane science* **2013**, *428*, 598–607.

(56) ElSherbiny, I.; Khalil, A. S. G.; Ulbricht, M. Influence of surface micro-patterning and hydrogel coating on colloidal silica fouling of polyamide thin-film composite membranes. *Membranes* **2019**, *9* (6), 67.

(57) Kim, I.; Choi, D.-C.; Lee, J.; Chae, H.-R.; Hee Jang, J.; Lee, C.-H.; Park, P.-K.; Won, Y.-J. Preparation and application of patterned hollow-fiber membrane bioreactor for wastewater treatment. *J. Membr. Sci.* **2015**, *490*, 190–196.

(58) Yoo, C. H.; Jo, Y.; Shin, J. H.; Jung, S.; Na, J.-G.; Kang, T.; Lee, J. S. Hierarchical membrane integration of shear stress-resistant nanoparticles and biomimetic micropatterns for ultrahigh and durable biofouling resistance. *Chemical Engineering Journal* **2022**, *432*, 134363.

(59) Zhao, Z.; Liu, B.; Ilyas, A.; Vanierschot, M.; Muylaert, K.; Vankelecom, I. F. J. Harvesting microalgae using vibrating, negatively charged, patterned polysulfone membranes. *Journal of membrane science* **2021**, *618*, 118617.

(60) Zhao, Z.; Muylaert, K.; Szymczyk, A.; Vankelecom, I. F. J. Enhanced microalgal biofilm formation and facilitated microalgae harvesting using a novel pH-responsive, crosslinked patterned and vibrating membrane. *Chemical Engineering Journal* **2021**, *410*, 127390.

(61) Zhao, Z.; Muylaert, K.; Vankelecom, I. F. J. Combining patterned membrane filtration and flocculation for economical microalgae harvesting. *Water research* **2021**, *198*, 117181.

(62) Mazinani, S.; Al-Shimmery, A.; Chew, Y. J.; Mattia, D. 3D printed nanofiltration composite membranes with reduced concentration polarisation. *Journal of membrane science* **2022**, *644*, 120137.

(63) Al-Shimmery, A.; Mazinani, S.; Ji, J.; Chew, Y. M. J.; Mattia, D. 3D printed composite membranes with enhanced anti-fouling behaviour. *J. Membr. Sci.* **2019**, *574*, 76–85.

(64) Mazinani, S.; Al-Shimmery, A.; Chew, Y. M. J.; Mattia, D. 3D Printed Fouling-Resistant Composite Membranes. *ACS Appl. Mater. Interfaces* **2019**, *11* (29), 26373–26383.

(65) Shang, C.; Wang, L.; Xia, J.; Zhang, S. Macropatterning of microcrumpled nanofiltration membranes by spacer imprinting for low-scaling desalination. *Environ. Sci. Technol.* **2020**, *54* (23), 15527–15533.

(66) Wang, S.; Wang, Z.-y.; Xia, J.-z.; Wang, X.-m. Polyethylene-supported nanofiltration membrane with in situ formed surface patterns of millimeter size in resisting fouling. *Journal of membrane science* **2021**, *620*, 118830.

(67) Vogelaar, L.; Barsema, J. N.; van Rijn, C. J. M.; Nijdam, W.; Wessling, M. Phase Separation Micromolding—PS $\mu$ M. *Adv. Mater.* **2003**, *15* (16), 1385–1389.

(68) Won, Y.-J.; Choi, D.-C.; Jang, J. H.; Lee, J.-W.; Chae, H. R.; Kim, I.; Ahn, K. H.; Lee, C.-H.; Kim, I.-C. Factors affecting pattern fidelity and performance of a patterned membrane. *Journal of membrane science* **2014**, *462*, 1–8.

(69) Maruf, S. H.; Li, Z.; Yoshimura, J. A.; Xiao, J.; Greenberg, A. R.; Ding, Y. Influence of nanoimprint lithography on membrane structure and performance. *Polymer* **2015**, *69*, 129–137.

(70) Maruf, S. H.; Greenberg, A. R.; Ding, Y. Influence of substrate processing and interfacial polymerization conditions on the surface topography and permselective properties of surface-patterned thin-film composite membranes. *Journal of membrane science* **2016**, *512*, 50–60.

(71) Weinman, S. T.; Fierce, E. M.; Husson, S. M. Nanopatterning commercial nanofiltration and reverse osmosis membranes. *Sep. Purif. Technol.* **2019**, *209*, 646–657.

(72) Ward, L. M.; Shah, R. M.; Schiffman, J. D.; Weinman, S. T. Nanopatterning Reduces Bacteria Fouling in Ultrafiltration. *ACS ES&T Water* **2022**, *2* (9), 1593–1601.

(73) Vogelaar, L.; Lammertink, R. G.; Barsema, J. N.; Nijdam, W.; Bolhuis-Versteeg, L. A.; van Rijn, C. J.; Wessling, M. Phase separation micromolding: a new generic approach for microstructuring various materials. *Small* **2005**, *1* (6), 645–655.

(74) Bikel, M.; Punt, I. G.; Lammertink, R. G.; Wessling, M. Micropatterned polymer films by vapor-induced phase separation using permeable molds. *ACS Appl. Mater. Interfaces* **2009**, *1* (12), 2856–2861.

(75) Ilyas, A.; Hartanto, Y.; Lee, L. C.; Vankelecom, I. F. J. Micro-patterned cellulose triacetate membranes for forward osmosis: Synthesis, performance and anti-fouling behavior. *Desalination* **2022**, *542*, 116076.



- (76) Ilyas, A.; Madhav, D.; Nulens, I.; Agrawal, K. V.; Van Goethem, C.; Vankelecom, I. F. Influence of micro-patterned support properties and interfacial polymerization conditions on performance of patterned thin-film composite membranes. *J. Membr. Sci.* **2024**, *700*, 122721.
- (77) Hutflés, J.; Chapman, W.; Pellegrino, J. Roll-to-roll nanoimprint lithography of ultrafiltration membrane. *J. Appl. Polym. Sci.* **2018**, *135* (11), 45993.
- (78) Chou, S. Y.; Krauss, P. R.; Renstrom, P. J. Imprint of sub-25 nm vias and trenches in polymers. *Appl. Phys. Lett.* **1995**, *67*, 3114–3116.
- (79) Chou, S. Y.; Krauss, P. R.; Renstrom, P. J. Imprint Lithography with 25-Nanometer Resolution. *Science* **1996**, *272*, 85–87.
- (80) Lyu, Z.; Ng, T. C. A.; Tran-Duc, T.; Lim, G. J. H.; Gu, Q.; Zhang, L.; Zhang, Z.; Ding, J.; Phan-Thien, N.; Wang, J. 3D-printed surface-patterned ceramic membrane with enhanced performance in crossflow filtration. *J. Membr. Sci.* **2020**, *606*, 118138.
- (81) Choi, W.; Jeon, S.; Kwon, S. J.; Park, H.; Park, Y.-I.; Nam, S.-E.; Lee, P. S.; Lee, J. S.; Choi, J.; Hong, S.; et al. Thin film composite reverse osmosis membranes prepared via layered interfacial polymerization. *J. Membr. Sci.* **2017**, *527*, 121–128.
- (82) Park, S.-J.; Lee, J.-H. Fabrication of high-performance reverse osmosis membranes via dual-layer slot coating with tailoring interfacial adhesion. *J. Membr. Sci.* **2020**, *614*, 118449 DOI: 10.1016/j.memsci.2020.118449.
- (83) Huang, S.; Mansouri, J.; McDonald, J. A.; Khan, S. J.; Leslie, G.; Tang, C. Y.; Fane, A. G. A novel single-scan printing approach for polyamide membranes by electrospray technique on polydopamine pre-coated substrate. *J. Membr. Sci.* **2023**, *673*, 121461.
- (84) Huang, S.; Mansouri, J.; Le-Clech, P.; Leslie, G.; Tang, C. Y.; Fane, A. G. A comprehensive review of electrospray technique for membrane development: Current status, challenges, and opportunities. *J. Membr. Sci.* **2022**, *646*, 120248.
- (85) Chung, J. Y.; Lee, J. H.; Beers, K. L.; Stafford, C. M. Stiffness, strength, and ductility of nanoscale thin films and membranes: a combined wrinkling-cracking methodology. *Nano Lett.* **2011**, *11* (8), 3361–3365.
- (86) Denizer, D.; ElSherbiny, I. M. A.; Ulbricht, M.; Panglisch, S. Studying Fluid Characteristics Atop Surface Patterned Membranes via Particle Image Velocimetry. *Chemie Ingenieur Technik* **2021**, *93* (9), 1401–1407.
- (87) Guillen, G. R.; Pan, Y.; Li, M.; Hoek, E. M. V. Preparation and Characterization of Membranes Formed by Nonsolvent Induced Phase Separation: A Review. *Ind. Eng. Chem. Res.* **2011**, *50* (7), 3798–3817.
- (88) Lau, W. J.; Ismail, A. F.; Goh, P. S.; Hilal, N.; Ooi, B. S. Characterization Methods of Thin Film Composite Nanofiltration Membranes. *Separation & Purification Reviews* **2015**, *44* (2), 135–156.
- (89) Horstmeyer, N.; Lippert, T.; Schön, D.; Schleder, F.; Picoreanu, C.; Achterhold, K.; Pfeiffer, F.; Drewes, J. E. CT scanning of membrane feed spacers-Impact of spacer model accuracy on hydrodynamic and solute transport modeling in membrane feed channels. *J. Membr. Sci.* **2018**, *564*, 133–145.
- (90) Benecke, J.; Haas, M.; Baur, F.; Ernst, M. Investigating the development and reproducibility of heterogeneous gypsum scaling on reverse osmosis membranes using real-time membrane surface imaging. *Desalination* **2018**, *428*, 161–171.
- (91) Jung, S. Y.; Ahn, K. H. Transport and deposition of colloidal particles on a patterned membrane surface: Effect of cross-flow velocity and the size ratio of particle to surface pattern. *Journal of membrane science* **2019**, *572*, 309–319.
- (92) Jung, S. Y.; Won, Y.-J.; Jang, J. H.; Yoo, J. H.; Ahn, K. H.; Lee, C.-H. Particle deposition on the patterned membrane surface: Simulation and experiments. *Desalination* **2015**, *370*, 17–24.
- (93) Jang, J. H.; Lee, J.; Jung, S.-Y.; Choi, D.-C.; Won, Y.-J.; Ahn, K. H.; Park, P.-K.; Lee, C.-H. Correlation between particle deposition and the size ratio of particles to patterns in nano- and micro-patterned membrane filtration systems. *Sep. Purif. Technol.* **2015**, *156*, 608–616.
- (94) Shang, W.; Yang, S.; Liu, W.; Wong, P. W.; Wang, R.; Li, X.; Sheng, G.; Lau, W.; An, A. K.; Sun, F. Understanding the influence of hydraulic conditions on colloidal fouling development by using the micro-patterned nanofiltration membrane: Experiments and numerical simulation. *Journal of membrane science* **2022**, *654*, 120559.
- (95) Malakian, A.; Zhou, Z.; Messick, L.; Spitzer, T. N.; Ladner, D. A.; Husson, S. M. Understanding the role of pattern geometry on nanofiltration threshold flux. *Membranes* **2020**, *10* (12), 445.
- (96) Lee, Y. K.; Won, Y.-J.; Yoo, J. H.; Ahn, K. H.; Lee, C.-H. Flow analysis and fouling on the patterned membrane surface. *Journal of Membrane Science* **2013**, *427*, 320–325.
- (97) Choi, W.; Shin, M. G.; Lee, G. W.; Kim, D.; Yoo, C. H.; Lee, J. S.; Jung, H. W.; Lee, J.-H. Anisotropic biofouling behavior of sharkskin-patterned desalination membranes. *J. Membr. Sci.* **2023**, *683*, 121814.
- (98) Miller, D. J.; Araújo, P. A.; Correia, P. B.; Ramsey, M. M.; Kruithof, J. C.; van Loosdrecht, M. C.; Freeman, B. D.; Paul, D. R.; Whiteley, M.; Vrouwenvelder, J. S. Short-term adhesion and long-term biofouling testing of polydopamine and poly(ethylene glycol) surface modifications of membranes and feed spacers for biofouling control. *Water Research* **2012**, *46* (12), 3737–3753.
- (99) Sperle, P.; Wurzbacher, C.; Drewes, J. E.; Skibinski, B. Reducing the impacts of biofouling in RO membrane systems through in situ low fluence irradiation employing UVC-LEDs. *Membranes* **2020**, *10* (12), 415.
- (100) Vrouwenvelder, J.; Van Paassen, J.; Wessels, L.; Van Dam, A.; Bakker, S. The membrane fouling simulator: a practical tool for fouling prediction and control. *J. Membr. Sci.* **2006**, *281* (1–2), 316–324.
- (101) Von Der Schulenburg, D. G.; Vrouwenvelder, J.; Creber, S.; Van Loosdrecht, M.; Johns, M. Nuclear magnetic resonance microscopy studies of membrane biofouling. *J. Membr. Sci.* **2008**, *323* (1), 37–44.
- (102) Sim, L. N.; Chong, T. H.; Taheri, A. H.; Sim, S. T. V.; Lai, L.; Krantz, W. B.; Fane, A. G. A review of fouling indices and monitoring techniques for reverse osmosis. *Desalination* **2018**, *434*, 169–188.
- (103) Verwey, E. J. W.; Overbeek, J. T. G. *Theory of the Stability of Lyophobic Colloids*; Dover Publications: New York, 1948.
- (104) Martines, E.; Csaderova, L.; Morgan, H.; Curtis, A. S. G.; Riehl, M. O. DLVO interaction energy between a sphere and a nano-patterned plate. *Colloids Surf., A* **2008**, *318*, 45–52.
- (105) Bendersky, M.; Davis, J. M. DLVO interaction of colloidal particles with topographically and chemically heterogeneous surfaces. *J. Colloid Interface Sci.* **2011**, *353*, 87–97.
- (106) Ducker, W. A.; Senden, T. J.; Pashley, R. M. Direct measurement of colloidal forces using an atomic force microscope. *Nature* **1991**, *353*, 239–241.
- (107) Bowen, W. R.; Doneva, T. A. Atomic Force Microscopy Studies of Membranes: Effect of Surface Roughness on Double-Layer Interactions and Particle Adhesion. *J. Colloid Interface Sci.* **2000**, *229*, 544–549.
- (108) Drechsler, A.; Petong, N.; Zhang, J.; Kwok, D. Y.; Grundke, K. Force measurements between Teflon AF and colloidal silica particles in electrolyte. *Colloids Surf., A* **2004**, *250*, 357–366.
- (109) Hoek, E. M. V.; Agarwal, G. K. Extended DLVO interactions between spherical particles and rough surfaces. *J. Colloid Interface Sci.* **2006**, *298*, 50–58.
- (110) Hoek, E. M. V.; Bhattacharjee, S.; Elimelech, M. Effect of Membrane Surface Roughness on Colloid-Membrane DLVO Interactions. *Langmuir* **2003**, *19*, 4836–4847.
- (111) Wang, M.; Wang, J.; Jiang, J. Membrane fouling: microscopic insights into the effects of surface chemistry and roughness. *Advanced Theory and Simulations* **2022**, *5* (1), 2100395.
- (112) Chevarin, C.; Wang, X.; Bouyer, D.; Tarabara, V.; Chartier, T.; Ayril, A. CFD-guided patterning of tubular ceramic membrane surface by stereolithography: Optimizing morphology at the mesoscale for improved hydrodynamic control of membrane fouling. *Journal of membrane science* **2023**, *672*, 121435.
- (113) Lin, W.; Wang, Q.; Liu, Z.; Meng, X.; Dai, P.; Huang, X. Improved hydrodynamic properties and enhanced resistance to

particle deposition and membrane fouling by millimeter-scale patterned membranes. *J. Membr. Sci.* **2024**, *700*, 122709.

(114) Yang, M.; Wang, J.; Zhang, M.; Liu, K.; Huang, H. Particle oscillation at corrugated membrane-water interface: An in-situ direct observation and implication to membrane fouling control. *Sep. Purif. Technol.* **2023**, *307*, 122835.

(115) Chauhan, D.; Nagar, P. K.; Pandey, K.; Pandey, H. Simulations of novel mixed-patterned membrane surfaces: Enhanced hydrodynamics and concentration polarization to mitigate fouling in water treatment. *Journal of Water Process Engineering* **2024**, *62*, 105371.

(116) Haaksman, V. A.; Siddiqui, A.; Schellenberg, C.; Kidwell, J.; Vrouwenvelder, J. S.; Picioreanu, C. Characterization of feed channel spacer performance using geometries obtained by X-ray computed tomography. *J. Membr. Sci.* **2017**, *522*, 124–139.

(117) Shang, C.; Xia, J.; Sun, L.; Lipscomb, G. G.; Zhang, S. Concentration polarization on surface patterned membranes. *AIChE J.* **2022**, *68* (12), No. e17832.

(118) Chauhan, D.; Nagar, P. K.; Pandey, K.; Pandey, H. Simulations of novel mixed-patterned membrane surfaces: Enhanced hydrodynamics and concentration polarization to mitigate fouling in water treatment. *Journal of Water Process Engineering* **2024**, *62*, 105371.

(119) Park, J. E.; Jung, S. Y.; Kang, T. G. Enhanced reverse osmosis filtration via chaotic advection induced by patterned membranes: A numerical study. *Desalination* **2023**, *565*, 116879 DOI: [10.1016/j.desal.2023.116879](https://doi.org/10.1016/j.desal.2023.116879).

(120) Shang, W.; Li, X.; Liu, W.; Yue, S.; Li, M.; von Eiff, D.; Sun, F.; An, A. K. Effective suppression of concentration polarization by nanofiltration membrane surface pattern manipulation: Numerical modeling based on LIF visualization. *Journal of Membrane Science* **2021**, *622*, 119021.

(121) Bucs, S. S.; Radu, A. I.; Lavric, V.; Vrouwenvelder, J. S.; Picioreanu, C. Effect of different commercial feed spacers on biofouling of reverse osmosis membrane systems: A numerical study. *Desalination* **2014**, *343*, 26–37.

(122) Yang, J.; Ma, Y.; Ma, C. Optimizing microstructure on surface of patterned membrane by smart algorithm and computational fluid dynamics. *Journal of Water Process Engineering* **2024**, *61*, 105264.

(123) Hu, J.; Harandi, H. B.; Chen, Y.; Zhang, L.; Yin, H.; He, T. Anisotropic gypsum scaling of corrugated polyvinylidene fluoride hydrophobic membrane in direct contact membrane distillation. *Water Res.* **2023**, *244*, 120513.

(124) Han, J.; Dai, P.; Gu, C.; Liao, Y.; Zhao, Y.; Razaqpur, A. G.; Sun, G.; Chou, S. Emulsified oily wastewater treatment via fertilizer drawn forward osmosis using a corrugated thin film composite membrane. *J. Membr. Sci.* **2023**, *685*, 121926.

(125) Tian, Y.; Dai, P.; Wu, B.; Liao, Y.; Gu, C.; Yang, T.; Li, X.; Li, X.; Feng, C.; Li, Y. Engineering a macro-corrugated composite membrane with superior anti-biofouling property for extractive membrane bioreactor. *Sep. Purif. Technol.* **2024**, *341*, 126926.

(126) Shang, C.; Pranantyo, D.; Zhang, S. Understanding the roughness-fouling relationship in reverse osmosis: mechanism and implications. *Environ. Sci. Technol.* **2020**, *54* (8), 5288–5296.

(127) Young, A. H.; Hotz, N.; Hawkins, B. T.; Kabala, Z. J. Inducing Deep Sweeps and Vortex Ejections on Patterned Membrane Surfaces to Mitigate Surface Fouling. *Membranes* **2024**, *14* (1), 21.

(128) Waters, J. T.; Liu, Y.; Li, L.; Balazs, A. C. Optimizing Micromixer Surfaces To Deter Biofouling. *ACS Appl. Mater. Interfaces* **2018**, *10* (9), 8374–8383.

(129) Gohari, R. J.; Lau, W. J.; Matsuura, T.; Ismail, a. Effect of surface pattern formation on membrane fouling and its control in phase inversion process. *Journal of Membrane Science* **2013**, *446*, 326–331.